13 Magnetospheric ULF Waves: A Review

Frederick W. Menk

Abstract

Ultra-low frequency (ULF; approx. 1 mHz $\leq f \leq$ 10 Hz) MHD plasma waves are readily recorded throughout the Earth's magnetosphere and on the ground. Generated by a variety of instabilities, ULF waves transport and couple energy throughout the system, and may play important roles in the energization and loss of radiation belt particles. ULF waves also provide a convenient probe and diagnostic monitor of the magnetosphere. The availability of multipoint measurements from spacecraft, ionospheric sounders and ground magnetometer arrays and the increasing sophistication of modeling tools have stimulated much recent progress in this area. Nevertheless, fundamental questions remain regarding the generation, propagation and consequences of these waves. This chapter reviews recent developments in these areas.

13.1 ULF Wave Sources

Ultra-low frequency (ULF) plasma waves are broadly of two types, depending on whether their energy source originates in the solar wind or from processes within the magnetosphere. Evidence for the former comes from the dependence of daytime power in the Pc3 (20–100 mHz), Pc4 (7–20 mHz) and Pc5 (1.7–7 mHz) ranges on solar wind speed and interplanetary magnetic field (IMF) clock angle (e.g. Odera 1986; Engebretson et al. 1987; Mathie and Mann 2001; Kessel et al. 2004; Francia et al. 2009). Solar wind density also plays an important role in controlling Pc3 activity (Heilig et al. 2010). Substorms and other instabilities in the tail form an important source of ULF waves on the nightside, but are considered elsewhere in this volume and the discussion here focuses on sources of waves on the dayside. Other recent reviews on ULF waves include Walker (2005), Kivelson (2006), Takahashi et al. (2006), Fraser (2007), and Villante (2007).

13.1.1 Sources in the Solar Wind

There are several ways in which ULF waves may be energized by the solar wind. A rich variety of plasma waves occurs in the magnetosheath, in particular Alfvén/ion cyclotron and mirror modes under low and high plasma β conditions respectively (Schwartz et al. 1996). Magnetospheric ULF waves occur most favorably under near-radial IMF conditions (Russell

F.W. Menk (✉)
School of Mathematical and Physical Sciences, The University of Newcastle, Callaghan, NSW 2308, Australia
e-mail: fred.menk@newcastle.edu.au

W. Liu, M. Fujimoto (eds.), *The Dynamic Magnetosphere*, IAGA Special Sopron Book Series 3,
DOI 10.1007/978-94-007-0501-2_13,

et al. 1983) when Alfvén/ion cyclotron waves may be produced upstream by the right-hand (RH) resonance instability with field-aligned backstreaming ions (Troitskaya et al. 1971; Takahashi et al. 1984; Le and Russell 1996; Blanco-Cano et al. 2009). Spatial properties of waves in the foreshock were described by Archer et al. (2005). The waves can convect downstream to the subsolar region of the magnetopause and into the magnetosphere without significant change to their spectrum (Greenstadt et al. 1983; Krauss-Varban 1994). The wave frequency depends on the strength and cone angle of the IMF but is typically in the Pc3 range (Takahashi et al. 1984).

Global two-dimensional hybrid (kinetic ions and fluid electrons) simulations for radial IMF conditions reveal the formation of a very perturbed foreshock region within which a slightly smaller ULF wave foreshock is embedded (Blanco-Cano et al. 2009). Weakly compressive sinusoidal waves in this region are RH polarized in the plasma frame but LH in the spacecraft frame. The extent of the foreshock over the dayside region decreases with increasing cone angle.

These ideas are supported by multisatellite observations of upstream waves entering and propagating through the magnetosphere as compressional waves (Sakurai et al. 1999; Constantinescu et al. 2007; Heilig et al. 2007; Clausen et al. 2008, 2009). By examining wavefront curvature and propagation properties for Pc3 waves recorded during an outbound magnetosheath crossing of the four Cluster satellites, Constantinescu et al. (2007) found that these waves mostly originated from the cusp and electron foreshock, but not especially from the ion fore-shock. This suggests that small Alfvén/ion cyclotron and mirror mode waves are initially stimulated in the electron foreshock and then couple to and are amplified by ion beam instabilities in the slightly downstream ion foreshock region.

In an independent study using the Cluster and Geotail spacecraft and ground magnetometers located near the Cluster footpoint, Clausen et al. (2009) found a 'cradle to grave' example of Pc3 event that was generated in the foreshock region after a sudden reduction in the solar wind cone angle, and was then observed in the outer magnetosphere and on the ground. The upstream waves were predominantly transverse but with a compressional component, relating (after a suitable propagation delay) to compressional waves in the outer magnetosphere that mode-converted to bandlimited field line guided toroidal Alfvén waves at the local field line eigenfrequency as verified using ground cross-phase measurements. The frequency of the upstream waves agreed precisely with the Takahashi et al. (1984) prediction.

Heilig et al. (2007) presented a detailed statistical survey of Pc3-4 compressional mode wave power at ~350 km altitude using the CHAMP spacecraft, finding that events between ±60° latitude are most likely generated in the upstream foreshock region, with wave frequency depending on IMF strength and a Doppler shift due to the Alfvénic mach number M_A, but not on the cone angle: $f_{peak}\,(\mathrm{mHz}) = (0.708 \cdot M_A + 0.64)\,(\mathrm{mHz/nT}) \cdot B_{IMF}\,(\mathrm{nT})$.

Periodic compressional or Alfvénic fluctuations in the solar wind may also directly drive discrete frequency ULF waves in the magnetosphere (e.g. Potemra et al. 1989; Prikryl et al. 1998; Stephenson and Walker 2002; Kepko and Spence 2003; Menk et al. 2003). Kessel (2008) examined the relationship between Pc5 wave power in the solar wind (ACE, Wind), near the magnetopause (Geotail), at geostationary orbit (GOES 8, 10), over the poles (Cluster), and on the ground near the Geotail and GOES footpoints, during high speed streams and coronal mass ejections. Over 80% of total Pc5 activity (including propagating compressional waves, field line resonances and global modes) during a 2 week interval was driven by solar wind pressure fluctuations, with the amplitude and power of Pc5 compressional fluctuations in the magnetosphere and on the ground being directly proportional to the amplitude and power of similar fluctuations in the solar wind.

A similar conclusion was reached by Takahashi and Ukhorskiy (2007, 2008) who conducted superposed epoch analyses of upstream solar wind parameters recorded by ACE, and Pc5 wave fields at GOES at solar maximum and solar minimum, finding that solar wind pressure variations are the major driver of Pc5 waves at geosynchronous orbit, where standing Alfvén waves are then established.

Recent event and statistical studies provide accumulating evidence that periodic variations in solar wind dynamic pressure are prompt drivers of some magnetospheric Pc5 ULF waves and field line resonances (FLRs) at the discrete 'magic' frequencies (0.7, 1.4, 2.0, 4.8 mHz) reported by Samson et al. (1992) and many others (e.g. Ziesolleck and McDiarmid 1994; Francia and Villante 1997) and ascribed to magnetospheric cavity/waveguide modes.

Examining a specific event, Fenrich and Waters (2008) used a phase coherence technique to show that 1.7 mHz oscillations in solar wind density were related, with 99% confidence and after a suitable propagation delay, to FLR signatures recorded near 62° magnetic latitude in the ionosphere with an HF SuperDARN radar. Villante et al. (2007) also used a phase coherence technique to examine the relationship between discrete frequency oscillations in the solar wind and at low latitudes on the ground, while Eriksson et al. (2006b) found that 9 out of 10 Pc5 events detected in the ionosphere by an HF radar exhibited high correlation coefficients with oscillations in the solar wind dynamic pressure. Such pressure-driven 'magic frequency' Pc5 pulsations can also be associated with auroral pulsations (Liou et al. 2008).

In an important study, Viall et al. (2009) examined the occurrence of discrete spectral peaks in the 0.5–5.0 mHz range for over 11 years of measurements of number density in the upstream solar wind (recorded by the Wind spacecraft) and for 10 years of magnetic field data in the magnetosphere within an hour of local noon (recorded by the geostationary GOES spacecraft). Using statistical tests on overlapping 6-h intervals, they found in both data sets discrete frequencies that occurred more often than other frequencies, and also determined that such discrete frequencies were seen in the magnetosphere 54% of the time they occurred in the solar wind. Their results are summarized in Fig. 13.1. The discrete frequencies are at or near the Samson 'magic' frequencies, although in both data sets there was some gradual evolution through the solar cycle. Viall et al. concluded that a clear physical relationship exists between some discrete, repeatable frequencies in solar wind number density and in the magnetosphere, although other discrete frequencies are also present in the magnetosphere due to other physical processes.

In conclusion, multipoint observations show that Pc3-4 ULF waves generated in the foreshock region

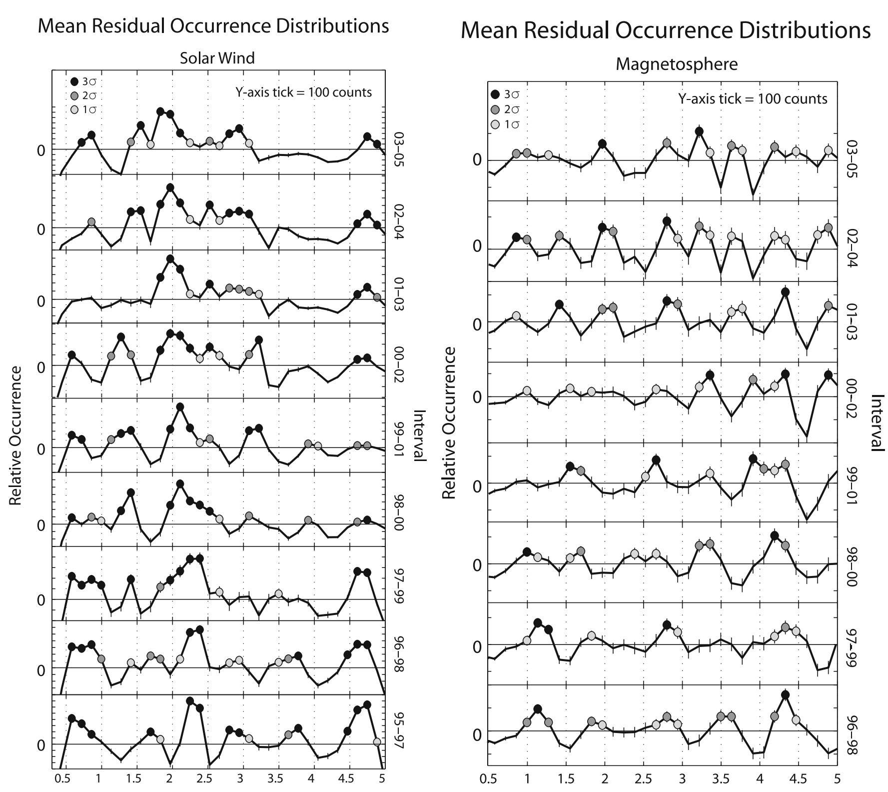

Fig. 13.1 Mean residuals of 3-year occurrence distribution of statistically significant frequencies over 1995–2005 in solar wind number density (*left*) and in the dayside magnetosphere (*right*). Vertical bars indicate ±1 s.d.; *y*-axis tick marks denote 100 counts (Figures 4 and 5 from Viall et al. 2009)

may be observed in the magnetosphere and on the ground, while there is also accumulating evidence that Pc5 waves may be directly driven by pressure oscillations in the solar wind. This may be an important source of magnetospheric ULF waves at low frequencies which are hard to reconcile with cavity/waveguide modes. Fundamental questions that arise include: (i) How important are these solar wind-related mechanisms as sources of Pc3-5 ULF waves in the daytime magnetosphere? (ii) Hence, how significant are cavity/waveguide modes? (iii) To what extent can these sources explain ULF waves seen on the ground in the polar cap and tail regions? (iv) Why and how should discrete frequencies be present in the solar wind?

13.1.2 Instabilities at the Magnetopause

The correlation between solar wind speed and ULF power in the magnetosphere suggests that the Kelvin-Helmholtz instability (KHI) resulting from the velocity shear at the magnetopause may be a significant source of ULF wave energy (e.g. Walker 1981; Pu and Kivelson 1983). The resultant surface waves propagate antisunward and are strongly evanescent within the magnetosphere. However, the shear flow between the plasma in the magnetosheath and magnetosphere also controls the reflection condition at the magnetopause, and when taking into account the boundary layer thickness this may result in the formation of over-reflection modes at the magnetopause (Mann et al. 1999; Walker 2000). Over-reflection occurs when the characteristic scales of the wave and the inhomogeneity are comparable, and may provide an efficient process for the extraction of energy from the magnetosheath to magnetospheric waveguide modes on the flanks during fast solar wind speed intervals (Wright and Mann 2006). This may explain the production of discrete frequency ULF waves in the magnetosphere and statistical correlations between Pc5 power on the ground and solar wind velocity (Mathie and Mann 2001; Mann et al. 2004; Pahud et al. 2009).

Numerical models now permit studies of the entire magnetosphere system under various conditions. Claudepierre et al. (2008) described a global three-dimensional (3-D) MHD simulation of the solar wind/magnetosphere interaction in which all solar wind parameters except driving velocity were held constant. Two coupled ULF surface modes were excited by the KHI near the dawn and dusk magnetopause, one propagating tailward along the magnetopause boundary and the other along the inner edge of the boundary layer. The phase velocities of the modes were different but the frequencies were the same and depended on the solar wind driving velocity. For both modes the preferred wavenumber was related to the boundary thickness, so that the KH waves are monochromatic.

Multispacecraft observations provide new opportunities for in situ studies of wave distributions and properties. Using 13 months' electric and magnetic field THEMIS data covering all local times but mostly under weak solar wind conditions, W. Liu et al. (2009a) found that wave power in the outer magnetosphere was greater in the Pc5 compared to the Pc4 range, being dominated by toroidal modes near the flanks and poloidal modes near noon. It was concluded that the KHI plays an important role in the excitation of Pc5 waves (especially near the flanks) during solar minimum years. During northward IMF conditions KHI events with particularly long wavelengths can be excited on the flanks of the equatorial magnetosphere (Hasegawa et al. 2009).

While Viall et al. (2009) suggested that solar wind perturbations drive ULF waves at certain frequencies, Plaschke et al. (2009a) presented results from an analysis of spline function interpolation of nearly 6700 THEMIS magnetopause crossings (to determine properties of magnetopause undulations) to suggest that Alfvénic waves propagating along the magnetopause surface may develop into standing Alfvén waves on the boundary due to reflection from the conjugate ionospheres (i.e. Kruskal-Schwarzschild modes). The surface waves are likely due to magnetopause displacements as a result of local pressure perturbations in the magnetosheath, while the eigenfrequencies of the standing modes are determined by the magnetopause geometry and are strikingly similar to the Samson 'magic' frequencies; see Fig. 13.2. Plaschke et al. (2009b) added solar wind observations to their dataset in order to determine the dependence of the observed spectrum of magnetopause oscillations on solar wind and IMF conditions and local time. They found that magnetopause oscillations occurred more favorably near noon and for northward IMF, low solar wind speed and low cone angle. This combination of conditions suggests that the oscillations are more likely

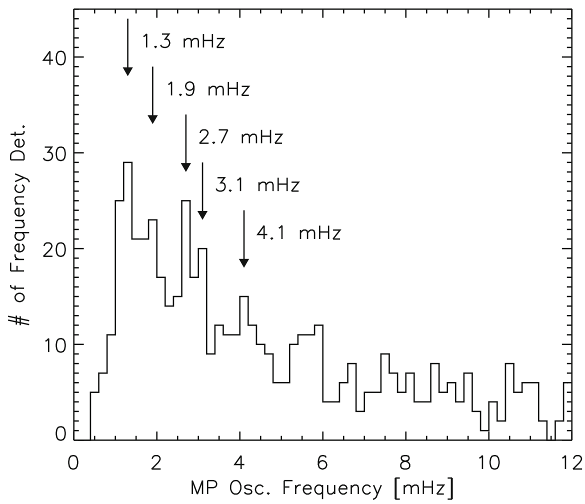

Fig. 13.2 Oscillation frequencies due to magnetopause motion (Figure 2 from Plaschke et al. 2009a)

due to Kruskal-Schwarzshild modes than solar wind pressure perturbations or the KHI at the flanks.

There have been few reports of the KHI in the magnetotail (e.g. Takagi et al. 2006). However, Volwerk et al. (2007) identified 5 min magnetic oscillations as the Cluster and Doublestar spacecraft entered a flow shear channel in magnetotail. The oscillations propagated Earthward at about half the plasma flow speed and increased in amplitude in agreement with KHI wave growth. These results also suggest that the KHI may play a role in the braking of fast flows in the magnetotail.

In conclusion, simulation and observational studies show that instabilities at the magnetopause are likely an important source of long period ULF wave activity. Further work is needed on both fronts to clarify the role of such instabilities as sources of 'everyday' wave activity. The significance of over-reflection and Kruskal-Schwarzshild modes requires particular investigation.

13.1.3 Interactions within the Magnetosphere

ULF waves can be generated by a variety of mechanisms internal to the magnetosphere, including drift-mirror instabilities due to pressure anisotropies, and drift-bounce resonance with trapped energetic ions (e.g. Walker 2005). These waves are often strongly compressional, have high azimuthal wave number, *m*, and are attenuated on the ground due to spatial integration, resulting in a 'hidden' wave population previously hinted at by radar observations (e.g. Yeoman et al. 2000) and fortuitous satellite conjunctions (e.g. Hughes et al. 1978). Recent radar observations are outlined in Section 13.4.

The drift-mirror instability occurs under high β conditions when there is significant perpendicular pressure anisotropy. The frequency of the growing mode depends on the diamagnetic drift frequency but the instability condition is affected by field line curvature and coupling to transverse shear Alfvén waves. The drift mirror waves will propagate slowly with the Larmor drift frequency. Rae et al. (2007) showed an example of a large amplitude compressional Pc5 wave event detected for some hours by Equator-S in the dawnside magnetopause under average solar wind conditions. The waves were most likely generated by a drift mirror instability near the equatorial plane and might also couple to local standing toroidal mode Alfvén waves.

High-*m* compressional Pc5 waves have been measured by the THEMIS spacecraft in the outer magnetosphere under average magnetic conditions near local dawn (Korotova et al. 2009) and dusk (Constantinescu et al. 2009). Both studies found the waves had wavelengths of ~2 R_E and propagated sunward at velocities of ~10–20 km/s, and both studies concluded that the waves were most likely generated by the drift mirror instability.

The availability of multipoint spacecraft observations has therefore provided new information on the source and generation of high-*m* waves in the outer magnetosphere.

13.2 Wave Generation and Propagation Mechanisms

The propagation of magnetospheric ULF plasma waves has been described in detail by many workers (e.g. Allan and Poulter 1992), usually in the context of standing shear Alfvén mode field line oscillations with low azimuthal wavenumber (e.g. Orr 1984) that are driven by energy coupling from incoming compressional fast mode waves (e.g. Odera et al. 1991). The latter may also excite global eigenoscillations of the magnetosphere (Kivelson and Southwood 1986; Allan et al. 1986a) or the plasmasphere (Allan et al. 1986b; Waters et al. 2000). In fact, the coupling of cavity or waveguide eigenmodes to FLRs may explain how discrete spectra are produced across a range of latitudes (Kivelson and Southwood 1985; Samson et al. 1995; Menk et al. 2000), including at the 'magic' frequencies (e.g. Samson et al. 1992; Mathie et al. 1996; Villante et al. 1997). However, cavity modes are difficult to detect with spacecraft (Waters at al. 2002) and the existence of highly stable discrete frequency modes is still controversial. On the other hand, the existence of a peculiar, large, highly monochromatic wave mode called giant pulsations has been known for a long time (e.g. Chisham et al. 1990). Measurements with ionospheric sounders have shown that these high *m* poloidal mode waves may be fairly common after storms (e.g. Wright and Yeoman 1999). In this section we focus mainly on waves generated in the local daytime.

13.2.1 Global Cavity Modes

Many studies have suggested that global cavity modes may be responsible for the appearance of ULF signals with multiple discrete spectral peaks at the 'magic' frequencies and spanning a range of latitudes. During very large storms such discrete frequency modes may be detected throughout the magnetosphere (Lee et al. 2007). Figure 13.3 shows discrete frequency Pc5

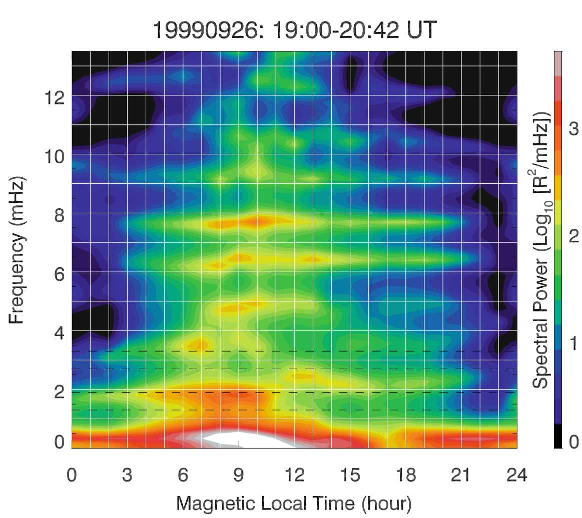

Fig. 13.3 Power spectrum of discrete frequency auroral pulsations. *Horizontal dashed lines* denote preferred Pc5 frequencies (Figure 2 from Liou et al. 2008)

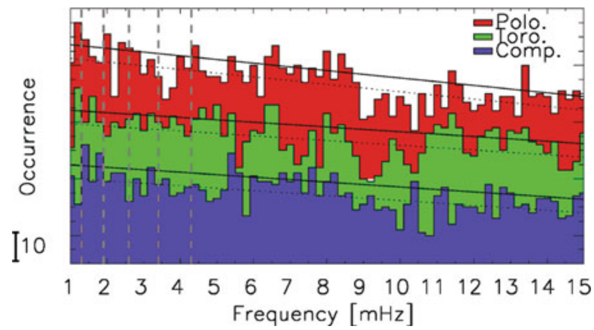

Fig. 13.4 Occurrence of spectral peaks in 1 year of Cluster magnetometer data (Adapted from Figure 11 of Clausen and Yeoman 2009)

pulsations and auroral modulations at frequencies up to 6–8 mHz, most likely produced by global cavity modes caused by solar wind pressure variations (Liou et al. 2008).

Using case studies and a 1-year statistical survey, Clausen and Yeoman (2009) examined FLRs recorded at the 'magic' frequencies by the Cluster spacecraft and at ground stations. As seen in Fig. 13.4, there was no preference for the set of 'magic' frequencies in the data, but there was a tendency for certain frequencies above 5 mHz, attributed to higher harmonics of waveguide/cavity modes.

Takahashi et al. (2009) reported the observation of global eigenmode oscillations near 15 mHz throughout the dayside plasmasphere (L~1.7–3.1) under conditions favorable for the propagation of broadband compressional mode power from the solar wind into the magnetosphere. However, no distinct plasmapause signature was evident and they therefore termed the plasmaspheric global mode a virtual resonance. The existence of such virtual resonance modes was predicted by Lee and Lysak (1999) and Lee and Takahashi (2006), and they are believed to account for the observed spectral properties of night-time Pi2 pulsations (Kim et al. 2005; Teramoto et al. 2008).

Plasmaspheric cavity resonances are expected to be a fraction of an R$_E$ apart (Samson et al. 1995), and it would be difficult to detect the resultant spectral fine structure using spacecraft, but this is easier with ground magnetometers. The structure of such trapped plasmaspheric modes was predicted using a simple 1-D waveguide model by Waters et al. (2000), confirming the observations of Menk et al. (2000). However, virtual resonance modes can extend beyond the plasmasphere and can exist even in the absence of a clear plasmapause boundary. Takahashi et al. (2005) pointed out that nightside Pc4 pulsations at geomagnetically quiet times could result from plasmaspheric cavity modes excited by a dayside energy source. Similar Pc4 pulsations have been reported in HF radar signals (Ponomarenko et al. 2003).

In summary, the following key questions remain unresolved. (i) Is there clear evidence in spacecraft data for the existence of cavity modes? (ii) Do cavity modes preferably exist at the 'magic' Samson frequencies or higher frequencies or both? (iii) Under which conditions do global cavity modes exist – i.e. extreme or quiet conditions; frequent or infrequent occurrence; dependence on a solar wind driver; etc? (iv) Under which conditions and at what frequencies do virtual cavity resonances exist compared to plasmaspheric cavity modes?

13.2.2 Field Line Resonances (FLRs)

The physical principles of FLRs are well known (e.g. Waters et al. 2006). However, mathematical descriptions often assume a simple dipolar geometry which is not appropriate to high latitudes where field lines experience significant temporal distortion. This affects the frequency (Waters et al. 1996; Wild et al. 2005) and polarization properties of the FLRs (Kabin et al. 2007). The latter is important because wave-particle energy transfer involves the wave electric field component parallel to the drift velocity of particle, i.e. the azimuthal field (poloidal mode) in a dipolar magnetic field. In order to obtain a more realistic representation of the situation Elkington et al. (2003) used a non-axisymmeteric compressed magnetic field model, but assumed that the wave electric field was either exactly radial or azimuthal. However, Kabin et al. showed that in a 3-D compressed dipole background field (described in terms of Euler potentials) and using the Rankin et al. (2006) standing shear Alfvén wave model, the polarization of Alfvén modes can no longer be described as poloidal or toroidal but becomes increasingly mixed and changes with local time. This arises because the contours of constant magnetic field no longer coincide with contours of constant wave period for either mode in the equatorial plane, as shown in Fig. 13.5. This means that at high latitudes different Alfvénic modes may contribute to particle acceleration in different MLT sectors.

This work has been extended by Degeling et al. (2010) who modeled the propagation of MHD waves and the formation of FLRs in a compressed dipole geometry including day/night asymmetry. In addition to the MLT dependence of shear Alfvén wave eigenmode polarization, they found that the FLR properties depend strongly on the wave source location at the magnetopause boundary.

A further complication arises when the magnetospheric plasma is in relative motion, such as near a KHI site. Kozlov and Leonovich (2008) modeled this analytically and numerically through azimuthal rotation of the plasma, finding that monochromatic fast magnetosonic waves could then excite harmonics of standing Alfvén waves simultaneously on different resonant surfaces. The plasma motion effect is greatest near strong density gradients (magnetopause, plasmapause) and results in distorted phase and amplitude profiles.

Sarris et al. (2009a, c) examined the structure of FLRs in situ between 4 R_E and the magnetopause using the THEMIS constellation. The polarization characteristics of the observed FLRs were in striking agreement with the Kabin et al. (2007) predictions based on a non-axisymmetric field geometry.

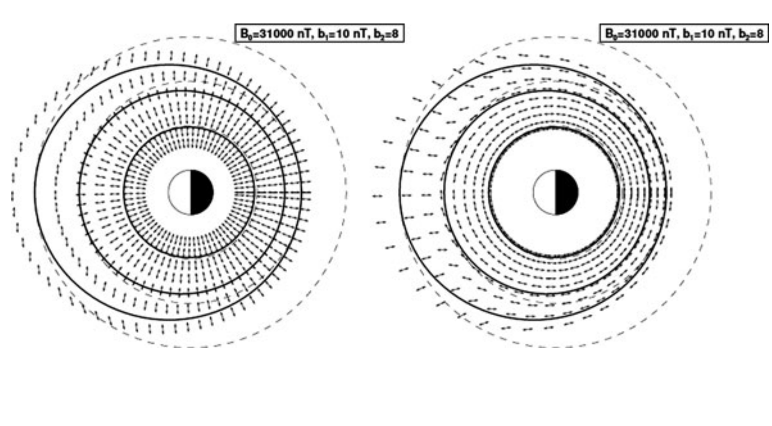

Fig. 13.5 Electric field polarization in the equatorial plane with a realistic magnetic field geometry and for the wave mode with radial electric field at midnight (*left*) and azimuthal field at midnight (*right*) (Figure 6 from Kabin et al. 2007)

Combined in situ observations with the 4 Cluster satellites and ground magnetometer measurements show (Liu et al. 2008) that Pc3 pulsations just inside the cusp have dominant transverse toroidal and poloidal components, wavelength $\sim 10^3$ km, and phase velocity $\sim 10^2$ km/s Earthward. The Poynting flux is field aligned and away from the equatorial plane. These waves likely arise from incoming compressional mode waves coupling to guided Alfvén waves on the last closed field lines, exciting FLRs at lower latitudes. In a follow-up study Y. Liu et al. (2009b) showed that the transverse scale size of these Pc3 waves near the cusp is ~ 0.14 R_E when using a threshold inter-spacecraft coherency of 0.65. There was also clear evidence of rotation of the polarization ellipse by 90° between the spacecraft and ground.

How much energy does a FLR deposit into the ionosphere? Estimates for large Pc5 FLR events include $\sim 6 \times 10^9$ W (Greenwald and Walker 1980), 10^{10}–10^{13} J (Allan and Poulter 1984), and 10^{10}–10^{11} J for high-m particle-driven FLRs (Baddeley et al. 2005a). Most recently, through combined Polar spacecraft, ground magnetometer and HF radar observations Rae et al. (2007) found that the energy dissipated into the ionosphere via Joule heating for a high solar wind speed-driven global Pc5 event was 10^{14}–10^{15} W, i.e. 30% of a substorm budget and much higher than previous estimates.

At low latitudes the source of FLRs is generally believed to be fast mode waves that propagate from the solar wind deep into the magnetosphere (e.g. Yumoto and Saito 1983; Yumoto et al. 1985; Matsuoka et al. 1997). The frequency of FLRs reverses near $L = 1.6$ due to ionospheric mass loading (Menk et al. 2000; Ndiitwani and Sutcliffe 2010), and the low latitude limit of FLRs is $L \approx 1.3$. In fact, recent observations have shown that discrete frequency fast mode waves are often present in the plasmasphere and couple to standing poloidal and toroidal modes causing FLRs that are detected on the ground (Menk et al. 2006; Ndiitwani and Sutcliffe 2009). In the former study poloidal mode flux tube oscillations at $L = 2.5$ were detected with VLF sounders, and coupled to FLRs that were recorded by ground magnetometers. The frequency of these signals corresponded with the frequency expected for waves generated in the upstream solar wind, although other discrete frequencies were also present in the spectra. The latter study used CHAMP low-Earth orbit spacecraft and ground magnetometer observations to show that discrete frequency fast mode oscillations above the ionosphere coupled to toroidal mode FLRs.

In summary, although the fundamental properties of FLRs are well known, many key questions still exist: (i) How do the properties of FLRs change at high latitudes in realistic field geometries? (ii) What is the effect of such changes (e.g. modified wave polarization) on particle acceleration? (iii) How significant is the effect of plasma motion on the properties of FLRs? (iv) There has been much discussion of the azimuthal wavenumber k_y. What are typical values for the meridional wavenumber k_x in FLRs? (v) How often do large FLRs occur that deposit significant energy into the ionosphere, and what are typical integrated values of energy deposition? (vi) What is the contribution of FLRs to the ULF wave spectrum at low latitudes? (vii) At high latitudes Pc3 signals are detected with clear FLR-like properties, with apparent poleward propagation (Howard and Menk 2005). Are these higher harmonics of FLRs, and if so what is the contribution of these to general ULF activity at high latitudes?

13.2.3 Other Alfvén Modes

Here we are concerned with poloidal mode waves, and coherent waves at high latitudes whose generation and propagation mechanisms are unclear. The compressional narrowband Pc4-5 waves described in Section 13.1.3 that are produced by drift-bounce resonance with trapped energetic ions have high azimuthal wave number m and induce poloidal mode (radial) field line perturbations. Most previous knowledge of these comes from HF radar measurements of wave fields in the ionosphere. Multipoint spacecraft observations are providing new information on these waves, which may persist up to days in the outer magnetosphere in the noon/postnoon sectors during the recovery phase of storms (Takahashi et al. 1985; Eriksson et al. 2005, 2006a; Sarris et al. 2007, 2009b; Schäfer et al. 2007, 2008). The waves are usually quite localized radially and have azimuthal wavenumbers as high as $m \sim 150$ (Eriksson et al. 2006a; Schäfer et al. 2008). The polarization of wave packets may also vary with time or spacecraft position, as predicted by Kabin et al. (2007).

Occasionally these waves are seen at quiet times when no energetic particles are present and drift or bounce resonance is unlikely (Eriksson et al. 2005). Sometimes high-m Pc4 waves are seen near the

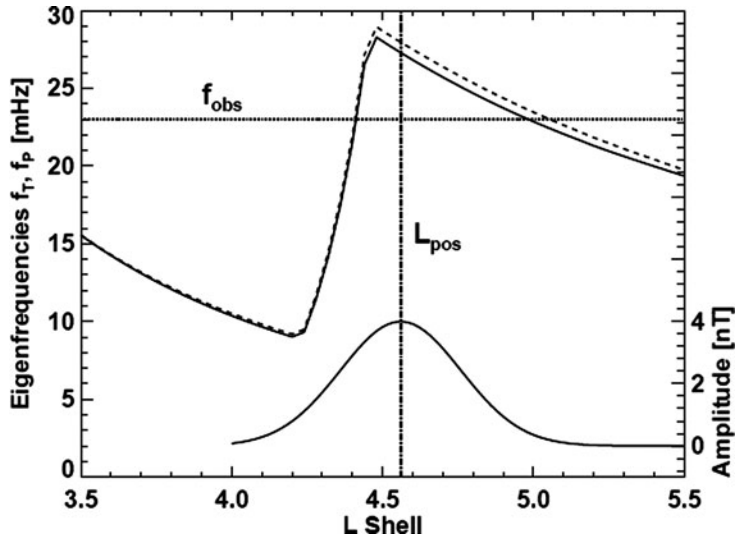

Fig. 13.6 Location of poloidal mode resonance region at the plasmapause. *Upper solid* and *dashed curves* show radial profiles of toroidal and poloidal mode eigenfrequencies; *horizontal dotted line* shows observed frequency $f_{obs} = 23$ mHz, and lower curve represents amplitude profile (Figure 14 from Schäfer et al. 2008)

plasmapause, suggesting they may be due to harmonics of poloidal mode eigenoscillations in a radially confined Alfvén resonance region at the inner (Schäfer et al. 2007) or outer edge of the plasmapause (Schäfer et al. 2008; Turkakin et al. 2008). This situation is illustrated schematically in Fig. 13.6 and was predicted by Klimushkin (1998). This is a new result not evident in ground records.

Observations of whistler mode waves with VLF sounders are sensitive to localized radial motions of flux tubes and show that poloidal mode field line oscillations are fairly common at quiet times, are related to fast mode ULF waves generated in the upstream solar wind, and couple to FLRs (Andrews 1977; Yearby and Clilverd 1996; Menk et al. 2006).

Questions that arise regarding new results on poloidal modes include: (i) How frequently do high-*m* poloidal mode particle-generated waves occur? (ii) Can such waves be generated at quiet times in the absence of energetic particle distributions? (iii) How common are high-*m* poloidal mode waves at the plasmapause and are they a signature of the plasmapause? (iv) What is the significance of these waves for the energization of ring current particles (see e.g. Ozeke and Mann 2008)? (v) Techniques such as VLF sounders and HF radars provide the possibility of ground-based monitoring of high-*m* poloidal mode waves. What new results could emerge?

An unresolved question is how coherent narrowband Pc3-4 waves arrive on open field lines in the polar regions (e.g. Santarelli et al. 2007); these signals may not just be a poleward extension of mid-latitude activity but relate to compressional waves in space (e.g. Engebretson et al. 2006). Pilipenko et al. (2008) suggested these pulsations may be due to the interaction of propagating magnetosonic and Alfvén waves. In a longitudinally inhomogeneous plasma the field-aligned wave vector components of travelling fast magnetosonic waves and Alfvén modes match, and fast mode energy may be resonantly converted to the latter. This may happen at frequencies much higher than the Alfvén resonance frequency.

An unexplained phenomenon is the existence of coherent low *m* waves that propagate sunward, away from the midnight sector. These have been observed in mid-latitude ground data (e.g. Mier-Jedrzejowicz and Southwood 1979) and now at large *L* with spacecraft (e.g. Erikkson et al. 2008). The latter reported observations of 1–2 mHz $m = 3$ toroidal waves at $L = 16$ post-midnight, with sunward propagation and Poynting flux, and wave frequency that changes with magnetic field strength. Wright and Allan (2008) reported numerical simulations of MHD wave coupling in the magnetotail waveguide that suggested 5–20 min fast mode waves generated in the magnetotail waveguide by substorms may couple to Earthward propagating Alfvén waves and produce field-aligned currents resulting in narrow auroral arcs that move equatorward at ~1 km/s. The Alfvén waves phasemix as they propagate Earthward, resulting in a rapid variation of wave fields perpendicular to *B*. The predicted wave properties agree with observations of Alfvén waves with local standing wave signatures in the PSBL and on the ground (Keiling et al. 2005). In summary, these new results raise the following questions: (i) What is the source of coherent narrowband Pc3-4 waves in the polar caps? (ii) What is the source of coherent sunward propagating waves in the tail? (iii) How common are such waves? (iv) Can mechanisms such as that proposed by Wright and Allan play a role in the generation of these waves?

13.3 Electromagnetic Ion-Cyclotron Waves (EMICWs)

Until recently the origin of magnetospheric Pc1-2 (∼0.2–5 Hz) waves was thought to be well understood. The waves are generally believed to be generated in the equatorial magnetosphere by ion-cyclotron resonance with unstable distributions of energetic ring current ions (e.g. Cornwall 1965; Criswell 1969) during the recovery phase of magnetic storms (Wentworth 1964). The characteristic fine structure appearance of 'pearl' Pc1 waves was attributed to dispersive field-aligned wave packet propagation in the LH ion mode on successive bounces between hemispheres (e.g. Jacobs and Watanabe 1964; Obayashi 1965). Non-propagation stop-bands occur at the local bi-ion frequencies in He^+ and O^+ rich plasmas (Fraser 1982). On reaching the ionosphere some of the wave energy couples to the RH mode and propagates in a horizontal waveguide centered on the ionospheric F2 region (Tepley and Landshoff 1966; Manchester 1970; Erlandson and Anderson 1996) from the source region near the plasmapause (e.g. Altman and Fijalkow 1980; Webster and Fraser 1985). IPDP are an unstructured subtype of Pc1-2 pulsations generated by resonant interaction with westward drifting energetic protons near the plasmapause in the evening sector (e.g. Horita et al. 1979). Figure 13.7 gives a schematic overview of the generation and propagation of structured Pc1 emissions.

Difficulties with the above picture of Pc1-2 generation were summarized by Demekhov (2007) and Mursala (2007), the main problem being lack of evidence of wave packet bouncing between conjugate points (Mursala et al. 1997). Spacecraft measurements have shown that EMICW propagation is almost exclusively away from the equator (Erlandson et al. 1996; Fraser et al. 1996) at latitudes greater than about 11° (Loto'aniu et al. 2005), with minimal reflection at the ionosphere. Furthermore, EMIC emissions can

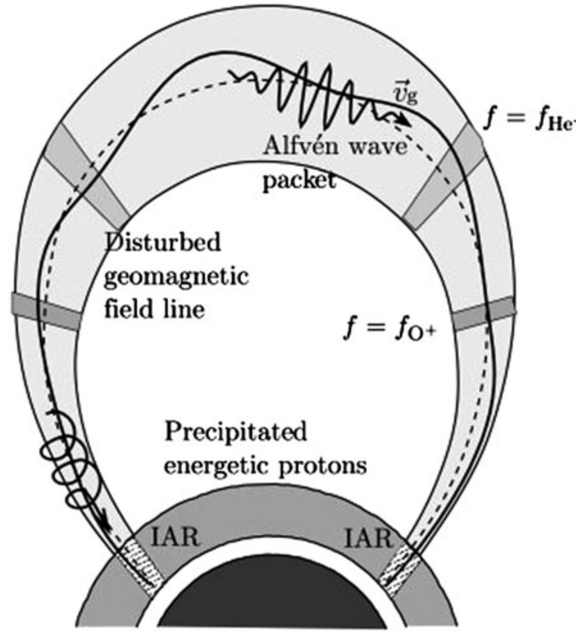

Fig. 13.7 Schematic picture of a magnetospheric flux tube in which Pc1 EMICWs are generated and propagate to the ground (Figure 2 from Demekhov 2007)

occur in the outer magnetosphere (Menk et al. 1992, 1993) in connection with solar wind perturbations (e.g. Olson and Lee 1983; Hansen et al. 1992, 1995; Arnoldy et al. 2005).

13.3.1 Observational Studies

Recent studies combining multipoint ground and in situ observations have confirmed that Pc1 EMICWs occur in localized L shells near the plasmapause (Usanova et al. 2008; Engebretson et al. 2008b) and are seen on the ground mostly after moderate and intense storms (Bortnik et al. 2008a; Engebretson et al. 2008a). The Usanova et al. study focused on emissions associated with a magnetospheric compression, detected by the THEMIS spacecraft in a narrow L range directly at the plasmapause, and with no evidence of wave packets bouncing back and forth to the ground. This work is important in the context of EMICW-particle interactions discussed later. The Bortnik et al. study examined 8 years of low latitude data using the automated detection algorithm mentioned in Section 13.5.4.

The association of EMICWs with energetic particle precipitation is reviewed in Section 13.5.3. Several authors have suggested that subauroral proton spots may be caused by pitch angle scattering by EMICWs generated by the interaction between hot ring current protons and cold plasmaspheric ions (e.g. Fuselier et al. 2004) or the enhanced cold dense plasma associated with plasmaspheric plumes (Frey et al. 2004; Spasojević et al. 2004). A direct connection between proton aurora spots, which map to the vicinity of the plasmapause, and EMICWs was demonstrated by Yahnin et al. (2007).

A statistical study by Engebretson et al. (2008a) reinforced the likely association between Pc1-2 on the ground in the recovery phase of storms and plasmaspheric plumes and precipitating energetic particles.

A complete 'cradle-to-grave' case study of EMIC wave propagation was presented by Morley et al. (2009). They used conjunction observations in the equatorial magnetosphere, at low-Earth orbit, and on the ground, to study the propagation of a LH polarized EMIC wave from the source region to the ground in association with > 6 keV ion precipitation. They also used a 2½-D MHD model to clarify the observed travel times, showing that the wave and ion source region was at the edge of a plasma drainage plume.

An important question in the discussion of EMICW generation and the particular packet structure that gave rise to the bouncing wave packet idea, is the possibility that the wave generation process is modulated by compressional Pc5 ULF waves. This has been confirmed by case studies and a statistical analysis of data from CRRES (Loto'aniu et al. 2009). They found a good linear correlation between Pc1 wave packet duration and Pc5 wave period, shown in Fig. 13.8, although the wave packets were sometimes 180° out of phase and non-adiabatic and non-linear processes may play a role.

During very intense storms unusually polarized Pc1-2 waves may be produced, including purely compressional waves near the equator that propagate radially Earthward, and waves with power in the radial and compressional but not azimuthal components that may propagate oblique to *B* (Engebretson et al. 2007).

Pc1-2 waves in the plasmasheet have components perpendicular and parallel to the field and propagate perpendicular to it (Broughton et al. 2008). Counterstreaming ion beams are also associated with these waves. At high latitudes, near the cusp, Pc1-2 signals often have the appearance of discrete bursts and structured emissions whose distribution is indicative of the source region and magnetospheric topology (e.g. Menk et al. 1992; Dyrud et al. 1997; Engebretson et al. 2009). Such Pc1-2 bursts accompany most magnetic impulse events (Arnoldy et al. 1996; Kurazhkovskaya et al. 2007), which are common in the polar regions (e.g. Sibeck and Korotova 1996).

In summary, while the general properties of Pc1-2 EMICWs are well established, the relative importance of sources associated with compressions, plasma plumes, or the ring current, and the significance of source modulation by Pc4-5 waves, remain unclear. Evidence for bouncing wave packets is also lacking.

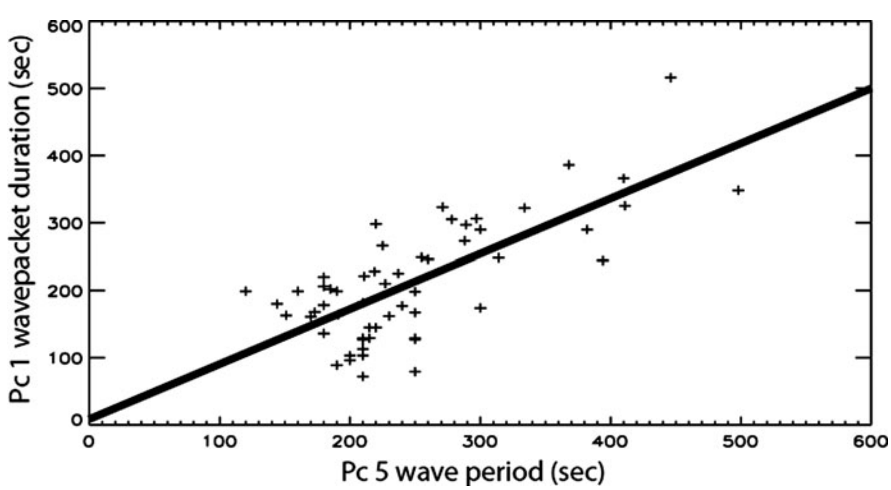

Fig. 13.8 Relationship between period of Pc1 wave packets and compressional Pc5 waves simultaneously seen at CRRES (Figure 6a from Loto'aniu et al. 2009)

13.3.2 Modeling and Simulation Studies

Recent modeling efforts have focused on clarifying the locations and conditions for EMICW generation, including the effect of heavy ion populations, and explaining the modulated appearance of wave packets. The competing generation models were reviewed by Demekhov (2007), with no clear consensus on a dominant mechanism. These are important questions since EMIC waves may control the precipitation of energetic ions (Jordanova et al. 2007) and relativistic electrons (Rodger et al. 2008). EMIC waves propagate across the Earth in the ionospheric Alfvén resonator, although the extent to which this determines the wave properties is unclear (Demekhov 2007).

Plasma density is one of the most important parameters controlling EMIC wave generation. Growth models which assume the total plasma is dominated by thermal plasma may not relate to regions where both cold plasmaspheric plasma and ring current ions are important. This situation was considered by Gamayunov and Khazanov (2008) using a global RC-EMIC simulation model referenced to plasma conditions observed during a large storm (but ignoring O^+ ions) and an analytical formulation of the Volland-Stern electric field. Their approach included wave growth, damping, propagation, refraction, reflection, and tunneling and showed that including the contribution of ring current H^+ in both the imaginary and real parts of the He^+-mode dispersion relation leads to the production of EMICWs where the suprathermal ($\leq$1 keV) ion fluxes are enhanced and the temperature anisotropy of energetic (>10 keV protons) is high. This agrees with observations by Engebretson et al. (2007) and suggests that suprathermal plasma plays a role in destabilizing the more energetic ring current and/or plasma sheet distributions to a high energy anisotropy.

Gamayunov and Khazanov (2008) also found that the results of Loto'aniu et al. (2005) are best explained by a model which assumes the EMICW source is at the equator and that waves reflect at off-equatorial latitudes at the bi-ion hybrid frequencies in conjugate hemispheres. Gamayunov et al. (2009) extended this modeling to incorporate M-I coupling including the magnetospheric electric field, ring current, plasmasphere and ionosphere. Figure 1 in their paper (not shown here) describes their approach in block diagram form. Initial simulations using this model, for the 2–4 May 1998 magnetic storm, showed that it would be necessary to extend the modeling domain to at least 72° latitude, to include a self-consistent description of the ionospheric conductance and the plasmasphere (e.g. plume structure).

In order to explain their observations that EMICW propagation is bidirectional within 11° of the magnetic equator but downward for |MLat|>11° Loto'aniu et al. (2005) suggested that EMICWs could be generated by a backward wave oscillator (BWO) in which waves generated at the equator are reflected back into this region by mirrors off the equator (not the heavy ion resonance locations), allowing feedback wave growth. This idea has been supported by quantitative modeling by Trakhtengerts and Demekhov (2007) for a threshold flux density of $\sim 10^7$ cm^{-2} s^{-1} for protons with energy $\geq$100 keV, and characteristic wave amplitude $\sim$0.01 nT at L=6.

Further information on the role of heavy ion hybrid resonances near the equator comes from modeling by Lee et al. (2008). By solving the full wave equations for a cold plasma they found that at resonance mode conversion occurs and the fast mode wave energy is absorbed, depending on the direction of the incident waves. Waves at resonance have linear polarization but the wave amplitude and frequency depend on the plasma composition. Fraser and McPherron (1982) had earlier discussed the effect of heavy ion resonance propagation effects in EMICW spectra.

EMICWs are occasionally observed on the ground with varying dispersion characteristics. Feygin et al. (2007) showed that events with falling frequency tones are due to RH magnetosonic waves, and a combination of R- and L-mode (i.e. EMIC) waves which produce mixed frequency dispersion. The R-modes may be due to cyclotron instability with 10–100 keV proton beams moving at $v_0 \geq U\|$ along the background field, where U is the thermal proton velocity in the beam. When $v_0/U\| << 1$ L-waves result. It should be noted that R-mode waves also occur on the ground due to mode conversion at the crossover frequency and tunneling at heavy ion stop bands (e.g. Rauch and Roux 1982).

The effect of heavy ion populations drifting relative to each other is to change the nonlinear dispersion relation for ICWs, leading to linear ion-acoustic instabilities and destabilizing nonlinear ion-acoustic waves (Gomberoff 2008).

The effect of Pc3-4 waves in modulating Pc1 EMICW growth rates was considered briefly in Demekhov (2007), who showed that for typical cold plasma conditions at $L = 7$ a ± 5 nT compressional wave can vary the gain over large ranges above and below the equatorial He^+ gyrofrequency, but at lower L values much larger wave amplitudes are required.

Recently interest has also focused on whether Pc1 EMICWs are excited at plume boundaries. Jordanova et al. (2007) used a global kinetic model including a time-dependent plasmasphere to determine the EMIC growth rate with time. They found the waves were preferentially excited in regions where energetic ring current populations, plumes and steep density gradients overlap. Ray tracing calculations by Chen et al. (2009) of ICW growth in a multicomponent cold storm-time plasma incorporating a realistic plasmasphere and a plume, and an additional bi-Maxwellian hot ring current distribution, found strong wave growth near the plasmapause, in density structures within the plume, and in the low density trough.

The Usanova et al. (2008) observations of compression-related EMICW activity have been modeled by McCollough et al. (2009) using a 3-D test particle solver coupled to the time-dependent MHD fields produced by the global LFM code. This allows a range of effects including solar wind compressions to be included. They found that after a compression wave growth was expected between $L = 5$–7 in the morning sector, and near the plasmapause at most times, in agreement with observations, and that the growth rate depends not just on warm plasma temperature anisotropies but also on warm and cold plasma densities (c.f. Gamayunov and Khazanov (2008) results above).

In summary, while important progress has been made with modeling studies of EMICW generation and propagation, the following questions remain: (i) Is there a favored mechanism for Pc1 pearl formation, or a combination of mechanisms at different times? (ii) What are the implications of these new modeling approaches for the scattering of ring current ions and relativistic electrons by EMICWs?

13.4 The Ionosphere Boundary

The conducting ionosphere forms the inner boundary of the magnetospheric cavity and therefore controls not only the formation and properties of standing field line oscillations (e.g. Dungey and Southwood 1970; Hughes, 1974; Yarker and Southwood 1986; Menk et al. 1995), but also the properties of cavity modes (Kivelson and Southwood 1985). In addition, all ULF waves observed on the ground propagate through the ionosphere and are therefore affected by its properties. The best known effect is the rotation of the polarization azimuth of the downgoing wave (Nishida 1964; Hughes 1983). The fields of these propagating waves can affect the ionospheric density distribution, thereby modifying ionospheric properties. These effects can be detected with HF radars and other sounders, and may modify the total electron content along GPS signal paths.

13.4.1 Effects of the Ionosphere on ULF Waves

We consider first recent theoretical treatments and observational results regarding effects of the ionosphere on FLRs, and waves in the Pc1 range. Waters et al. (this volume) provide a more detailed treatment of the underlying principles.

MHD models now being used to investigate the effects of ionospheric conductivity on FLRs incorporate a realistic ionosphere, oblique magnetic fields, and a mixture of incident wave modes. Sciffer and Waters (2002) presented an analytic description of this form, including a reflection and wave mode conversion coefficient matrix to describe mixing and conversion between shear Alfvén and fast mode energy at the ionosphere and atmosphere. These properties were found to depend critically on the perpendicular wavenumber *ky*. This formulation was extended by Sciffer et al. (2004) to include an inductive shielding effect for oblique magnetic fields (and hence high to low latitudes). This effect arises from the generation of an 'inductive' rotational current by the induced part of the divergent electric field in the ionosphere, reducing the wave amplitude detected on the ground.

Using a 1-D numerical formulation Sciffer et al. (2005) found that for an oblique magnetic field the rotation of the wave polarization azimuth depends on the compressional mode characteristics and the mode conversion and reflection properties from the ionosphere. Waters and Sciffer (2008) described a 2-D MHD formulation which was used to investigate the dependence of FLR frequency on ionospheric conductivity. They found that under typical mid/low latitude summer and winter conditions the FLR frequencies change by less than 5%. However, at auroral latitudes it is necessary to account for ionospheric feedback arising from changes in the Pedersen conductivity due to electron precipitation. Lu et al. (2007) incorporated a model of an active auroral ionosphere with a 2-D MHD model of the magnetosphere using both dipolar and stretched field geometries. They found that ionospheric feedback effects can produce strongly localized FLRs and enhanced amplitudes.

Direct observations of low-mid latitude Pc3-4wave structure with the CHAMP spacecraft and simultaneously on the ground below were described by Heilig et al. (2007) and Ndiitwani and Sutcliffe (2009). These confirm that Pc3-4 waves propagate through the magnetosphere mostly in the compressional mode and appear in the D component on the ground, coupling to discrete FLRs at the characteristic latitude, with 90° rotation in polarization of the signal on the ground.

This situation was confirmed by Pilipenko et al. (2008) using numerical modeling to calculate the relationship between Pc3 wave power above the ionosphere and on the ground. They also found that diurnal variations in the ionosphere/ground amplitude ratio do not depend strongly on ionospheric conductance, but the fast mode field is sensitive to the crustal surface conductivity.

At equatorial latitudes the nonuniform ionospheric conductivity at dawn results in strong changes in Pc3 amplitude and D component phase on the ground, although the phase of the H component is largely unchanged (Tanaka et al. 2007). It is not clear whether this results from the ionospheric effect on incident Alfvén or fast mode waves (cf. Waters et al. 2001).

New observations and modeling have confirmed the existence of quarter-mode FLRs near the dawn terminator, mostly in winter and summer in the US sector (Obana et al. 2008). These modes result from the asymmetry in ionospheric conductivity at conjugate points, and point to the need for caution in FLR-based magnetospheric density surveys. The difference in solar illumination at conjugate points also causes a strong seasonal asymmetry in plasmaspheric density that is maximum in US longitudes around $L = 2$–3 (Clilverd et al. 2007a).

In conclusion, new datasets and improvements in modeling the effect of the ionosphere are starting to provide a clear picture of the propagation of Pc3-4 signals to the ground. The question arises whether it is possible to characterize the ionospheric transfer function for incident ULF waves at all latitudes.

Consideration of ionospheric effects at Pc1 frequencies should incorporate the effect of the ionospheric Alfvén resonator (IAR). The IAR affects the spectrum of 0.1–10 Hz wave power reaching the ground (Belyaev et al. 1989; Demekhov et al. 2000) and at low latitudes is expected to be excited by lightning discharges. Properties of the IAR, including the diurnal variation, are determined mainly by the variation in Alfvén velocity at the F-layer peak (Hebden et al. 2005). Waters et al. (this issue) provide a detailed description of wave propagation in the IAR, pointing out the need to include magnetic inclination effects away from high latitudes. This changes the resonant frequency (Bösinger et al. 2002) and was described by Bösinger et al. (2009), who computed artificial power spectra of ULF fields at mid- and low-latitude ground sites. They found uneven harmonic spacing and separation in frequency of the Br and $B\varphi$ resonance components. Demekhov (2007) has outlined difficulties with the notion that the IAR determines the spectrum of Pc1 waves on the ground.

Simulations using a 3-D linear model of the propagation of kinetic Alfvén waves in the IAR in the presence of parallel and perpendicular density gradients (Lysak and Song 2008) reveal the formation of narrow-scale Alfvén waves which may be important in the auroral acceleration process. Figure 13.9 illustrates the Ex electric field component at various times after excitation. Interference between waves reflected from the ionosphere and the IAR leads to small scale structure that develops with time, and increases with increasing Pedersen conductance.

A statistical study of observations from the CHAMP spacecraft has revealed the existence of bursts of very intense kilometer-scale FACs in the auroral regions (Rother et al. 2007).

In summary, there is accumulating evidence on the formation and properties of the IAR, and while this may ultimately be important for some auroral processes, more work is required to clarify the role the IAR plays in determining the occurrence and properties of Pc1 pulsations on the ground across a range of latitudes.

13.4.2 Effects of ULF Waves on the Ionosphere

ULF wave fields drive perturbations in the ionosphere that may be detected with high frequency (HF) Doppler sounders (e.g. Menk et al. 1983; Menk 1992)

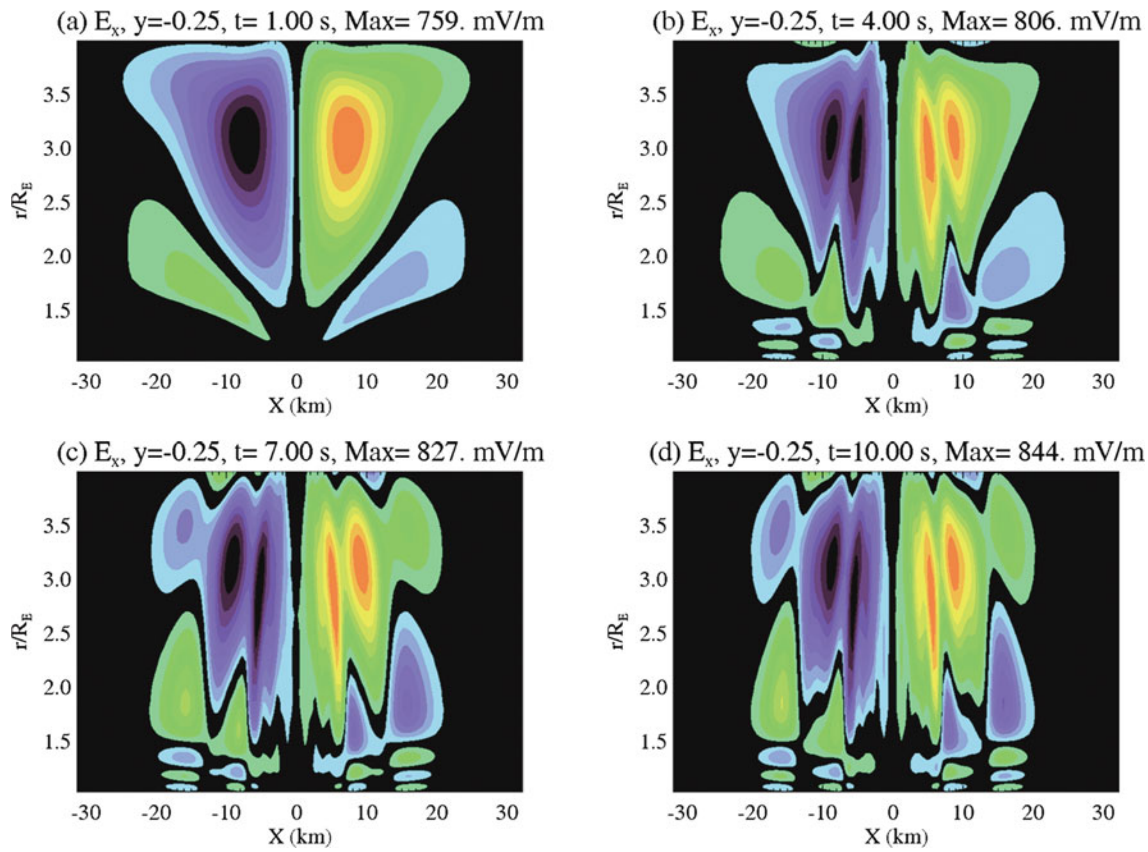

Fig. 13.9 *Ex* component of the electric field at 1, 4, 7 and 10 s after excitation by a 1 Hz 10 km wave field incident at 4 RE on a density cavity (Figure 2 from Lysak and Song 2008)

or HF radars (Ponomarenko et al. 2003) including the low latitude Arecibo radar (Ganguly and Behnke 1982). Doppler sounder measurements, in particular, have revealed the existence of a significant population of very high-m waves that is largely hidden from ground magnetometers (Wright et al. 1999; Wright and Yeoman 1999; Yeoman et al. 2000; Baddeley et al. 2005b). A very detailed review of new developments in HF radar science over the past decade was presented by Chisham et al. (2007).

The process by which Alfvén waves incident on and propagating through the ionosphere lead to ULF ionospheric Doppler oscillations was first described in detail by Poole et al. (1988) and Sutcliffe and Poole (1989). This was extended and generalized by Waters et al. (2007) to incorporate a mixture of downgoing wave modes and oblique magnetic field geometry, providing good agreement with observed Doppler shifts for an $m \sim 150$ and $m \sim 10$ event recorded by HF sounders near 66° latitude. The modeling is sensitive to the choice of wavenumber k_x and k_y and the incident wave mode mixture, but shows that the main contribution to the ionospheric Doppler shift arises from $e \times B_o$ advection motion of the ionospheric plasma driven by the ULF wave electric field.

Menk et al. (2007) reported a study of ULF Doppler oscillations in the ionosphere recorded with an array of HF sounders and ground magnetometers over $L = 1.56$–2.77. They examined the ionosphere-ground amplitude and phase relationship (see Fig. 13.10) for the perturbations as a function of frequency and latitude and compared these with the Waters et al. (2007) model predictions. As the incident wave mix changed from purely fast mode away from resonance to largely shear Alfvén mode at resonance, there was a pronounced change in the amplitude and phase of the ionospheric oscillations. In fact, at these low latitudes the ULF resonance structure was more clearly evident in the ionospheric sounder rather than the ground magnetometer signals.

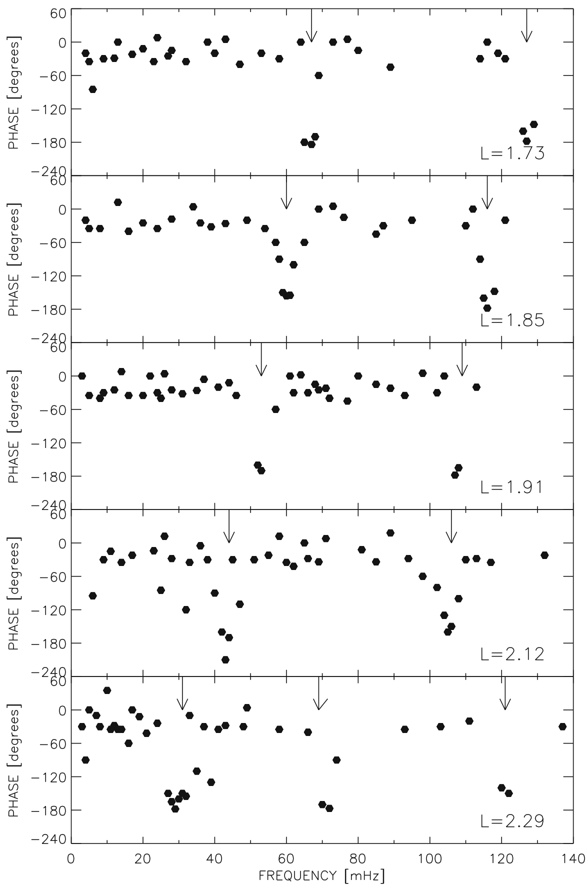

Fig. 13.10 Phase difference between ULF perturbations in the ionosphere and on the ground at low latitudes. *Arrows* indicated FLR frequencies and harmonics (Figure 2 from Menk et al. 2007)

An unusual result is the observation at $L = 1.3$ with the Arecibo radar of 1.7 mHz oscillations in ionospheric plasma frequency at two points 160 km apart in the F-region (Dyrud et al. 2008). The perturbation spectrum was qualitatively similar with GOES-10 magnetic field and WIND solar wind number density spectra, suggesting the ionospheric oscillations were caused by 'magic frequency' ULF waves propagating Earthward from the solar wind.

These results provide an interesting comparison with observations of 1.7–1.9 mHz oscillations by SuperDARN HF radars. Menk et al. (2003) showed that solar wind pressure variations in this range stimulated ULF waves and FLRs recorded by ground magnetometers, and ionospheric and ground scatter returns in high latitude HF sounder and radar signals. More recently, Mthembu et al. (2009) also reported the observation of 'magic' frequencies, in particular 1.9 mHz FLRs, in radar returns and in the upstream solar wind.

ULF waves also cause perturbations in the total electron content (TEC) of the ionosphere (Poole and Sutcliffe 1987; Karatay et al. 2010). The resultant time delays and phase shifts in HF signals propagating through the ionosphere affect GPS and radio astronomy operations (Skone et al. 2009; Waters and Cox 2009).

Mid-latitude radars can detect the ionospheric signatures of sub-auroral Pi2 pulsations associated with substorm expansion (Gjerloev et al. 2007). Comparison by them of the observed amplitude and phase relationships for a given event with the Sciffer et al. (2004) model suggests the incident wave is predominantly shear Alfvén mode wave with $m{\sim}2.3$. The measured and modeled perturbations are compared in Fig. 13.11.

The inverse process, the production of ULF waves through modification of ionospheric density with modulated RF transmissions, has been demonstrated on open field lines at 1.67 mHz (Clausen et al. 2008). It is also possible in this way to artificially enhance FLRs on closed field lines, through the production of an

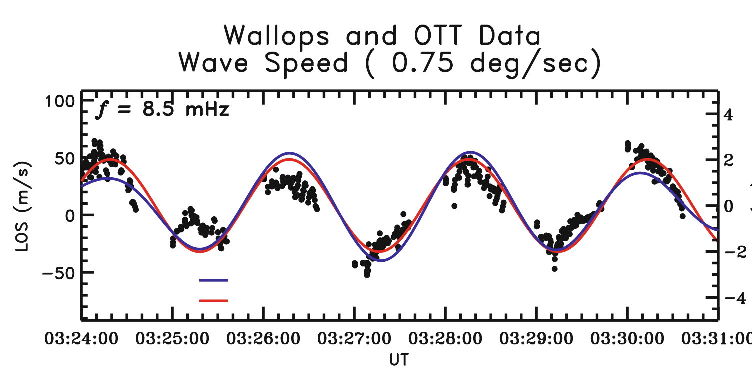

Fig. 13.11 Wallops HF radar line-of-sight drift velocities (*black dots*), ground magnetic field perturbation b_x (*blue*) and modeled ground field perturbation b_x (*red line*) for a mid-latitude Pi2 event (Figure 4 (*top*) from Gjerloev et al. 2007)

oscillating current system in the ionosphere (Badman et al. 2009). The resultant FLRs were detected by the Cluster spacecraft at ~11 R_E altitude. This is the first such report of field line 'tagging' by joint ground- and space-based techniques.

In conclusion, ULF field line signatures can be recorded in the ionosphere from low to high latitudes. In the latter case the waves may arise from solar wind pressure perturbations, or be triggered by substorms. Under appropriate assumptions of horizontal wave number and mode mix of the incident waves, relatively simple models can predict the resultant amplitude and phase profile reasonably well. Extension of these models to higher dimensions would provide more information on ULF wave properties at the ionosphere. It is clear, however, that ionospheric sounders can provide new information not available from magnetometers on ULF waves at the lower boundary of the magnetosphere-ionosphere system.

13.5 Consequences and Applications of ULF Waves

Since the Alfvén velocity depends on mass density and magnetic field strength, and since ULF waves propagate throughout the magnetosphere, they can be used as a diagnostic probe of magnetospheric density and hence structure, source region locations, and solar wind conditions (e.g. Obayashi and Jacobs 1958; Troitskaya 1961; Gul'yel'mi 1966; Troitskaya and Gul'yel'mi 1967, 1970). While much of the Earth's surface lies at low geomagnetic latitudes, the corresponding magnetic field lines map to a small fraction of the magnetospheric cavity which is difficult to study using spacecraft. Furthermore, due to charging effects it is difficult to measure the cold (< 1 eV) ion density that comprises the bulk of the inner magnetosphere population. Therefore ground-based observations are important for studying the inner magnetosphere (e.g. Menk et al. 1999, 2000). New analysis techniques including automated FLR detection algorithms facilitate such studies. At radiation belt altitudes particles can lose or gain energy via wave-particle interactions while waves are amplified or damped, and particles can be scattered into the loss cone and precipitate to low altitudes. Such interactions may have space weather consequences. It has also been suggested that some properties of ULF waves may be linked to seismic activity, and health effects.

13.5.1 Magnetospheric Remote Sensing

It has long been recognized that measurement of the eigenfrequency of magnetospheric field line resonances can provide information on the mass density threading the field line, mostly near the equatorial plane where the field-aligned Alfvén speed is a minimum (e.g. Obayashi and Jacobs 1958; Gul'yel'mi 1966; Poulter and Nielsen. 1982; Orr 1984). However, the distribution of plasma mass density along the field line alters the harmonic spacing of ULF resonances (Poulter et al. 1988; Takahashi et al. 2004) and mass loading due to heavy ions of ionospheric origin becomes important at low latitudes (Hattingh and Sutcliffe 1987; Waters et al. 1994). At high latitudes the field line geometry, and in particular the diurnal variation, plays an important role in determining the resonance frequency (Waters et al. 1995). Use of the dipole approximation introduces errors in mass density estimates for $L > \sim 3$ (Singer et al. 1981; Berube et al. 2006). The structure and location of Pc1-2 waves also provides a convenient diagnostic of high latitude topology (Menk et al. 1992). Ground based techniques for determining the FLR frequency were outlined in Menk et al. (1999).

There is growing use of ground ULF wave FLR observations to monitor magnetospheric properties such as the radial density distribution (Waters et al. 1996; Loto'aniu et al. 1999; Menk et al. 1999; Dent et al. 2003) and hence the plasmapause position (Milling et al. 2001; Menk et al. 2004; Dent et al. 2006), the presence and evolution of plasmaspheric plumes and biteouts (Abe et al. 2006; Grew et al. 2007; Takahashi et al. 2008), refilling processes (Dent et al. 2006; Obana et al. 2010), and the location of the open-closed field line boundary (Ables and Fraser 2005). Such remote sensing using ground-based observations of standing Alfvén waves is sometimes termed normal mode magnetoseismology (Chi and Russell 2005). Comparison with other techniques allows the plasma composition to be determined (Grew et al. 2007; Takahashi et al. 2008).

A statistical study of ULF field line resonance frequencies at low latitudes ($L < 2$) has demonstrated that the daily average FLR frequency, and hence plasmas-pheric mass density, follows the 27-day variation in $F_{10.7}$ solar flux with a 1–2 day time delay (Vellante et al. 2007). This shows that at low latitudes the FLR frequency is clearly controlled by the solar EUV irradiance, and the flux tubes may be regarded as being in diffusive equilibrium with the underlying ionosphere. Vellante et al. also noted a pronounced annual variation in mass density, which probably varies with longitude as determined for electron densities using VLF whistler measurements (Clilverd et al. 1991) and is probably due to the tilt of the magnetic dipole axis from the rotation axis. The existence of quarter-mode FLRs near the dawn terminator points to the need for caution in FLR-based magnetospheric density surveys (Obana et al. 2008).

It is interesting to compare FLR-derived estimates of mass density near the equatorial plane with independent determinations of electron density, which can be used to determine the heavy ion mass loading factor (Menk et al. 1999). In particular, due to mass loading effects the electron and heavy ion density profiles may be significantly different at the plasmapause or plume boundaries, especially in the presence of an O^+ torus (Fraser et al. 2005). Sometimes the dominance of heavy ions in the plasmatrough may mask the plasmapause and plasma plume boundaries compared to electron number density or light ion data (Takahashi et al. 2008).

An intercalibration of ULF-derived mass densities, electron densities from VLF whistler measurements and IMAGE spacecraft RPI data, and IMAGE EUV He^+ density estimates, was described by Clilverd et al. (2003). Grew et al. (2007) mapped the presence of a plume and biteout and showed that during an extended disturbed interval the H^+:He^+:O^+ composition by number in the plasmasphere and plasmatrough (near $L = 2.5$) was $\sim$82:15:3, but just outside the plasmapause the O^+ concentration exceeded 50%, suggesting the presence of an oxygen torus. Takahashi et al. (2008) compared mass density measurements based on in situ E and B field measurements from CRRES, with electron number densities measured by the same spacecraft, and found that in a plasma plume H^+ was the dominant species, while O^+ accounted for $\sim$90% of the mass density.

Earlier, Berube et al. (2005) had compared the FLR-based mass density between $L = 1.7$ and $L = 3.2$ with in situ plasmaspheric electron densities determined from the IMAGE RPI, finding that heavy ion concentrations were enhanced during large storms, when a heavy ion torus is likely to form. Mass density has been found to rapidly increase over $1.6 < L < 5.1$ immediately following a very large storm onset due to rapid outflow of ionospheric O^+ (Kale et al. 2009), followed by plasmaspheric density depletion and refilling for the next few days.

A detailed study of post-storm refilling using ground-based FLR observations was reported by Obana et al. (2010). They found that refilling takes 2–3 days for $L = 2.3$ flux tubes, 3 days at $L = 2.6$, and over 4 days for $L > 3.3$, and determined the upward plasma flux (at the 1000 km level) and the daily average refilling rate. Finally, by comparison with IMAGE-EUV and VLF whistler data they estimated the O^+ plasma concentration was of order 3–7% at $L = 2.3$ and 6–13% at $L = 3.0$.

The cross-phase technique (Waters et al. 1991) is perhaps the best-known method for determining toroidal mode FLR frequencies with closely-spaced ground stations. Kale et al. (2007) showed that where the radial density gradient exceeds r^{-8} (i.e. near a steep plasmapause) the cross-phase is reversed. Such cross-phase measurements all relate to the magnetic H component between meridionally spaced stations. Menk et al. (2006) demonstrated that the D component cross-phase may also provide information on poloidal mode resonances.

These methods rely upon knowledge of the field-aligned density distribution, which is often assumed to obey a power law (e.g. Cummings et al. 1969; Berube et al. 2005; Vellante and Förster 2006). This assumption, and improvements, have been discussed by many authors (e.g. Schulz 1996; Denton and Gallagher 2000). The spacing of FLR harmonics allows the mass density at points along the field line to be determined without assuming any functional form for the density distribution (Price et al. 1999). Satellite measurements of toroidal resonance harmonics near L=7 suggest that the field-aligned density distribution is better described by a polynomial series (Takahashi et al. 2004; Takahashi and Denton 2007), revealing an equatorial density enhancement in the afternoon sector at geostationary orbit and near 4.8 R_E (Denton et al. 2009) where density varies with L like L^{-4}. However, in many situations the simple power law approach allows the radial density profile to be estimated within observational uncertainty limits (Menk et al. 2004; Vellante and Förster 2006; Maeda et al. 2008).

In addition to using the eigenfrequency of standing Alfvén field line eigenoscillations to estimate mass density, it is also possible to estimate the density distribution and hence Alfvén speed required to explain the measured travel time of MHD waves through the magnetosphere and to the ground (Matsuoka et al. 1997; Chi et al. 2001; Howard and Menk 2001, 2005; Ponomarenko et al. 2005; Chi et al. 2006). The waves essentially obey Huygens' and Fermat's principles and follow the path that minimizes the travel time and conserves the most wave energy; this path involves fast mode MHD waves propagating initially Earthward in the equatorial plane and converting to field-aligned Alfvén waves. This is a fairly common concept in geophysics (e.g. Moser 1991) and explains why Pc3 ULF pulsations appear to propagate poleward across the ground at high latitudes (Howard and Menk 2005).

In conclusion, magnetoseismology offers the ability to remotely monitor magnetospheric properties including the plasmapause location, the radial density profile, and under certain conditions the presence of plasma plumes, the field-aligned density distribution, and the plasma composition. Measurements of the field line eigenfrequency and harmonics are the most established techniques for this, although the wave travel time can also provide information on the density distribution. Further intercalibration studies are required to compare ground-based mass density estimates with in situ observations in order to understand the full utility of the technique, and the precision of composition estimates. It would also be interesting to study how mass loading and hence plasma composition varies with magnetic activity and L.

13.5.2 Energization of Magnetospheric Particles

In recent years there has been considerable interest regarding the role and efficiency of ULF waves in accelerating trapped magnetospheric particles, especially in the radiation belts (e.g. O'Brien et al. 2003; Summers et al. 2007; Shprits et al. 2008a, b). A detailed review was presented by Elkington (2006).

Many observational studies have highlighted an association between Pc3-5 ULF waves and the energization of radiation belt electrons, particularly at geosynchronous altitude (e.g. Mathie and Mann 2001; O'Brien et al. 2003). In fact, long duration elevated Pc5 wave power seems to be a strong predictor of enhancements in relativistic electron fluxes at geosynchronous orbit (O'Brien et al. 2001). Statistically there is a strong correlation between solar wind speed, Pc5 ULF wave power and MeV electron fluxes throughout the outer radiation belt, with the highest correlations late in the declining phase of the solar cycle when the radiation belts are most intense (Mann et al. 2004). There is also a clear and systematic time lag, with MeV electron fluxes at geosynchronous altitudes lagging the peak in ULF wave power by $\sim$2 days, before peaking later at lower L shells.

Electron distribution functions in the radiation belts often peak at pitch angles perpendicular to the background field, and diffusive cross-L transport of electrons is believed to involve resonant interaction of the electron drift motion with ULF electric and magnetic field oscillations. Such processes violate the third adiabatic invariant and require the superposition of multiple stochastic interactions when averaged over a statistical ensemble incorporating different wave frequencies and phases, LT distribution, and variations in solar wind pressure (Ukhorskiy et al. 2005; Degeling et al. 2006; Elkington 2006).

Test-particle simulations have shown that perturbations in electric and magnetic fields are induced across wide regions of the magnetosphere by global magnetospheric compressions due to ULF variations in solar wind dynamic pressure and presumably also FLRs and magnetosonic waves (Ukhorskiy et al. 2006). Resonant interaction of the drift motion of electrons with these fields drives cross-L transport and radial diffusion in the inner magnetosphere, although the collective motion of outer belt electrons can exhibit large deviations from simple radial diffusion (Ukhorskiy and Sitnov 2008).

Diffusion models require the perpendicular electric and compressional magnetic diffusion coefficients to be specified in terms of ULF wave power. This means in turn that ground observations of ULF wave power need to be mapped to the equatorial plane. Analytical (e.g. Ozeke et al. 2009) and empirical/statistical (e.g. Brautigam et al. 2005) approaches may be used.

The average rate of radial diffusion is described by the diffusion coefficient and is a function of L, the wave power and mode structure. Time scales are typically of order a day (Elkington 2006). Loto'aniu et al. (2006) used ground magnetometer observations during a very large storm, when large amplitude ULF waves and relativistic electrons were recorded deep in the slot region ($L\sim2$–3), to calculate the in situ equatorial poloidal electric field PSD values and hence determine the radial diffusion rates. They found diffusion rates were 3–5 h at $L>4$ and 12–24 h for $L<4$, able to account for the observed increase in relativistic electrons in the slot. O'Brien et al. (2003) had earlier found during a solar cycle-long statistical survey that ULF activity is probably responsible for the main electron acceleration at geosynchronous orbit, but that VLF/ELF wave interactions were required to account for electron flux peaks at $L\sim4.5$.

The ULF waves responsible for radial transport of trapped electrons are often believed to be toroidal mode Pc5 waves such as FLRs with low azimuthal wavenumbers and radially directed electric field perturbations (e.g. Elkington et al. 2003; Ukhorskiy and Sitnov 2008; Degeling et al. 2008). In reality the waves usually exhibit a mixture of toroidal and poloidal modes (e.g. Ukhorskiy et al. 2005; Loto'aniu et al. 2006), and although the radial electric field of the toroidal component often dominates observations, diffusion rates due to the azimuthal electric fields of the associated poloidal modes are much more important (Ukhorskiy et al. 2005; Elkington 2006). Figure 13.12 shows results of numerical test particle simulations for 1 MeV electrons, compared to theoretical expectations, for $m=1$ ULF waves with azimuthal and radial electric fields based on a statistical survey of wave observations from CCRES. The required stochasticity in electron motion is assumed to arise due to randomness introduced by solar wind turbulence.

There have been concerns that radial diffusion cannot account for the relativistic particle fluxes that occur during storms (e.g. Horne et al. 2005). A non-diffusive mechanism for the energization of electrons by Pc5 ULF waves has been proposed by Degeling et al. (2006, 2008). This involves adiabatic transport due to drift resonance interaction between individual packets of coherent, narrowband compressional waves and equatorially mirroring MeV electrons, leading to localized peaks in electron phase space density. The initial time-dependent compressional waves may be launched from disturbances at the magnetopause, have low azimuthal wavenumber ($m\sim3$) in the magnetosphere, and couple to FLRs. The waves were modeled with an ideal MHD approach in a dipolar geometry and only azimuthal fields, well away

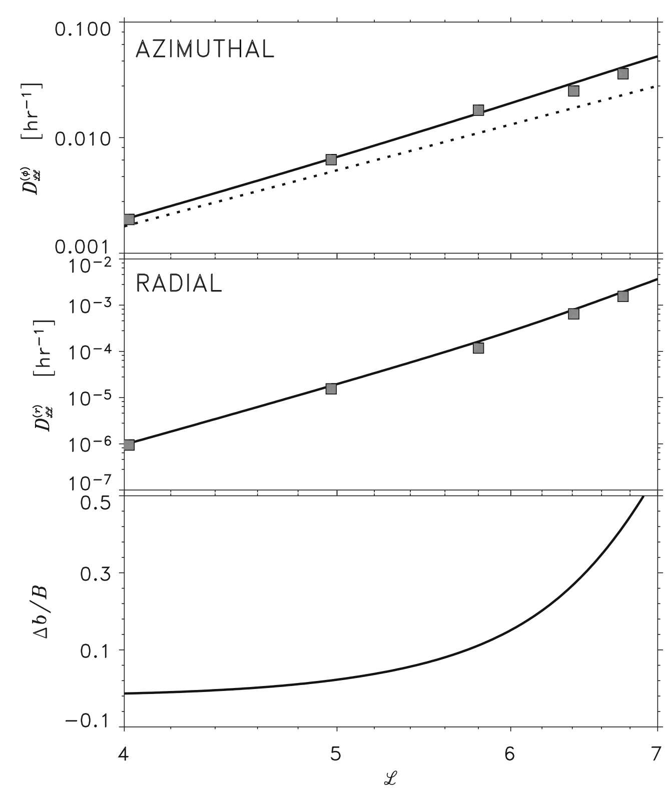

Fig. 13.12 Diffusion rates for 1 MeV equatorial electrons due to low m ULF waves. *Top*: azimuthal electric field; theoretical values shown with *solid lines*, and numerical values with *square symbols*. *Middle*: radial electric field. *Bottom*: background field asymmetry (Figure 5 from Ukhorskiy et al. 2005)

from the FLR, were considered. Because the wave phase speed and the azimuthal electron drift speed need to be similar, the drift resonance interaction region is limited to a range in *L* that depends on the wave amplitude.

While much attention has focused on low-*m* ULF waves, large amplitude internally generated high-*m* Pc4-5 waves also occur at storm times. Ozeke and Mann (2008) considered guided poloidal waves with mainly azimuthal electric fields and $m \geq 10$. The waves can be generated by the N=2 drift-bounce resonance interaction with energetic ring current ions (~10–15 keV H^+ or ~100–300 keV O^+). Such ion populations may occur in the inner magnetosphere at storm times when the plasmapause is at low *L*. The resultant waves have eastward phase propagation. In turn, eastward drifting >1 MeV radiation belt electrons may undergo drift resonance with the fundamental mode waves at $L \sim 3$–4. Note that the high-*m* poloidal waves could also be produced by other mechanisms, such as the Kelvin-Helmholtz instability, and are partially or largely screened from the ground due to spatial integration effects. This mechanism provides an interesting and potentially important process for particle energization at storm times.

The arrival of interplanetary shocks can stimulate high-*m* poloidal and toroidal waves throughout the magnetosphere, and Zong et al. (2009) used Cluster-Double Star observations to record the almost simultaneous enhancement of energetic electron fluxes in the radiation belt, probably due to drift-resonance acceleration by the waves.

Higher frequency plasma waves may accelerate radiation belt electrons through gyroresonant interactions. This includes EMIC waves (Summers et al. 2007) and fast magnetosonic waves with frequency below the lower hybrid resonance frequency but above the local proton gyrofrequency (i.e. in the range 20–60 Hz) (Horne et al. 2007). The waves are generated by ion ring distributions in the ring current at frequencies close to harmonics of the proton gyrofrequency, and interact with electrons and ions via the Doppler shifted cyclotron resonance. While it is generally believed that whistler mode chorus waves are very effective in accelerating electrons to MeV energies (e.g. Horne et al. 2005), Horne et al. (2007) suggested that magnetosonic waves may be equally important in accelerating these particles.

Recently attention has focused on the energization of auroral electrons by inertial Alfvén waves (e.g. Chaston et al. 2003; Seyler and Liu 2007). This topic is not reviewed here. Note however that the fluxes of energetic electrons and ions may be modulated by low-*m* standing toroidal mode Pc5 ULF waves in the outer magnetosphere, probably due to drift resonance interactions (Zong et al. 2007).

In conclusion, statistical and case studies show that ULF waves likely play a major role in the energization of relativistic particles in the radiation belts and into the slot. Questions remain concerning the relative contributions of different Pc5 wave types: radial diffusion due to broadband low-*m* waves, adiabatic transport due to time dependent compressional waves, and high-*m* waves in the ring current, as well as the role of EMIC waves.

13.5.3 Precipitation of Magnetospheric Particles

Many studies confirm that EMIC waves may cause pitch angle scattering and precipitation into the atmosphere of energetic protons (e.g. review by Yahnin and Yahnina 2007) and electrons (e.g. review by Millan and Thorne 2007).

Yahnin and Yahnina (2007) outlined observations demonstrating that localized precipitation of energetic protons is due to the scattering of particles into the loss cone by Pc1 ICWs in the equatorial plane. In the morning sector localized proton auroras may be connected with Pc1 sources associated with undulation of the plasmapause surface, while in the evening sector the waves may be generated near plasmaspheric plumes (e.g. Spasojević et al. 2004). Observations detailing the formation of an isolated subauroral proton arc (30–80 keV protons at $L \sim 4$) in the premidnight sector in association with intense Pc1 EMICWs near the plasmapause were presented by Sakaguchi et al. (2007).

There is accumulating observational evidence that EMIC waves are also responsible for relativistic electron precipitation (REP) after geomagnetic storms (e.g. Lorentzen et al. 2000; Meredith et al. 2003; Loto'aniu et al. 2006; Clilverd et al. 2007b; Blum et al. 2009). Examining an isolated proton aurora, Miyoshi et al. (2008) compared ground-based optical observations, co-located magnetometer measurements of associated Pc1 pulsations, and data from the POES-17 satellite as it passed over the ground stations showing precipitating 10s of keV ions and MeV electrons. DMSP mapped this region to the plasmapause. Miyoshi et al. were then able to demonstrate that the pitch angle diffusion coefficients were consistent with scattering of the relativistic electrons by the EMIC waves.

Results from a new and independent method for detecting REP were presented by Rodger et al. (2008), who have established a global network of VLF receivers which monitor the absorption of artificially produced VLF signals along a range of subionospheric paths. REP results in localized VLF absorption at altitudes below ∼70 km. Riometer absorption is weak or absent at these times. They detected such events near the plasmapause during small geomagnetic disturbances in association with IPDP/Pc1 EMIC activity recorded on ground based magnetometers.

There has also been considerable effort on modeling the process by which EMICWs scatter radiation belt electrons. This is usually regarded as a gyroresonance process and treated with a bounce-averaged quasi-linear diffusion approach (e.g. Summers et al. 2007). Jordanova et al. (2008) described a kinetic ring current-atmosphere interaction model (RAM) that includes radiation belt electron and ring current ion interactions with EMICWs whose excitation is incorporated self-consistently, and incorporates convective and diffusive transport and various loss processes. Using initial conditions referenced to observations and empirical models, they calculated the global precipitating electron and ion fluxes at 200 km altitude at various times during the large 21 October 2001 storm, finding that REP due to EMICWs maximized at $L\approx4.5$ near dusk at hour 18 but with localized patches elsewhere. Outward radial diffusion was the main loss process for $L>5$, while ion precipitation was most intense at low L shells at hour 24. Figure 13.13 summarizes their results, which compare favorably with observational studies mentioned above.

In contrast to gyroresonance scattering that violates the first invariant, Shprits (2009) pointed out that bounce resonance interaction with magnetosonic and EMIC waves, violating the second invariant, may be an important process for pitch-angle scattering of particles mirroring near the equator. It should be noted that the interaction between radiation belt electrons and EMICWs can be highly nonlinear (Albert and Bortnik 2009) and that the waves can be highly oblique (Khazanov and Gamayunov 2007).

13.5.4 New Techniques

As outlined earlier, there is growing use of ULF FLR measurements for magnetospheric remote sensing. The tedium of manually determining resonance frequencies and the existence of large ULF wave datasets has led to the development of automated detection algorithms (Berube et al. 2003; Vellante et al. 2007). An automatic algorithm to identify Pc1 wave events and

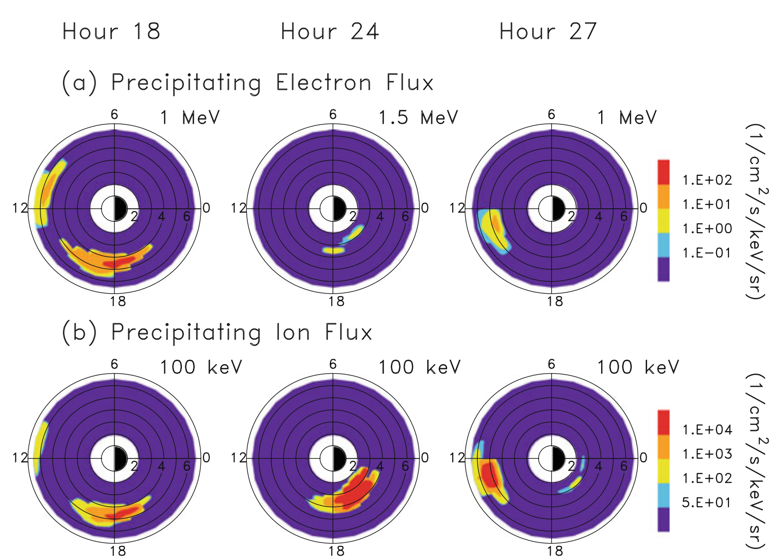

Fig. 13.13 Computed global distribution of energetic electron and ion number fluxes at selected times after 0000 UT on 21 October 2001 due to interactions with EMIC waves (Figure 6 from Jordanova et al. 2008)

simultaneously characterize their polarization properties has also been developed by Bortnik et al. (2007), who illustrated its use on 6 months of data. Their statistical analysis included the determination of cross-correlation for 12 wave parameters including wave frequency and bandwidth, azimuth angle, plasmapause location, and He^+ gyrofrequency.

The performance of FFTs to identify ULF waves in such procedures has been compared with wavelet transform (WT) techniques (Boudouridis and Zesta 2007; Heilig et al. 2007; Murphy et al. 2009), maximum entropy spectrum analysis (MESA; Ndiitwani and Sutcliffe 2009), Wigner-Ville distributions (WVD; Chi and Russell 2008), and Hilbert-Huang transforms (HHT; Kataoka et al. 2009). The FFT seems to outperform the continuous WT in automated FLR detection approaches (but the Morlet WT is better where the signal changes rapidly), while the WVD offers several advantages (especially for time-varying signals such as Pi2, Pc1 packets and phase skips in Pc3-4) including the ability to determine wave polarization properties. However, it is important to first detrend the data series and the WVD approach is more computationally intensive than the FFT or wavelet approaches. The HHT decomposes the waveform into a small number of intrinsic mode functions for which the instantaneous frequency is determined by the Hilbert transform. The method is particularly well suited for irregular signals such as Pi1, Pi2 and storm-time Pc3 packets.

The use of discrete wavelet transforms (DWTs) based on the Meyer wavelet for detecting Pi2 signals was first evaluated by Nosé et al. (1998). A detector and locator of substorm onsets based on Pi1/2 detection in this way was described by Milling et al. (2008) and Murphy et al. (2009). The first of these papers illustrated the use of the Meyer DWT to determine the onset time (resolution ∼16 s) and location of Pi1 activity at substorm onset, and the subsequent expansion rate. The locations of the upward and downward field aligned currents were also determined. The second paper validated the DWT technique by comparing ULF wave onset times and locations for 5 substorms and one pseudobreakup with IMAGE-FUV observations. Figure 13.14 shows an example for a substorm initiated over the CARISMA magnetometer array.

A 'wave telescope' field line resonance detector for multipoint data was described in detail by Plaschke et al. (2008). The technique estimates the spectral energy density of the wave field across a station array,

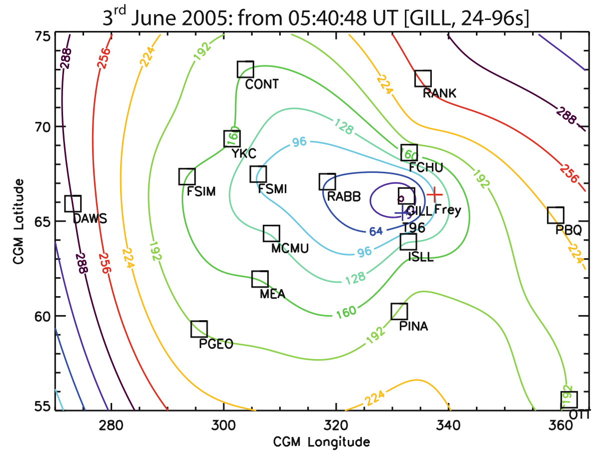

Fig. 13.14 Contours of Pi1/2-based onset times for a substorm on 3 June 2005 (Figure 6 from Murphy et al. 2009)

and is thus able to find hidden FLR phase structures because of the coherency across a large area. The use of the detector was demonstrated on 1 year of ground magnetometer data from the CARISMA array, where FLR properties such as time distribution, location, azimuthal wavenumber, see Fig. 13.15, were determined.

An important concern in magnetospheric physics is mapping ground-based observations to the magnetosphere. Ozeke et al. (2009) have shown analytically how to map magnetic field amplitudes observed on the ground, through the ionosphere, to electric field amplitudes in the equatorial plane for the guided toroidal and poloidal modes. They also compared numerical solutions with an observational example of a guided toroidal FLR, providing two simple expressions for

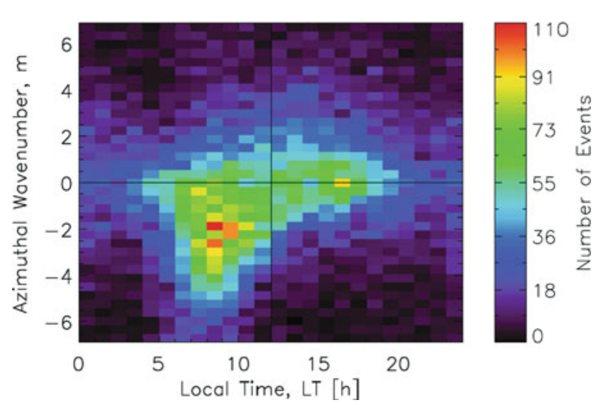

Fig. 13.15 Distribution of FLR events in 1 year of CARISMA ground data sorted by LT and azimuthal wavenumber (Figure 10 from Plaschke et al. 2008)

determining the ionospheric magnetic field and hence the equatorial electric field.

In conclusion, several important new techniques have been recently developed to facilitate the automatic detection of Pc1 ULF waves, Pi1 and Pi2 and hence substorm onsets, and FLRs, and for determining wave properties in space using ground instruments. These techniques should provide new opportunities for statistical and detailed case studies using existing and growing new datasets.

13.5.5 Other Effects

There have been reports for many years that Pc1 pulsations may be associated with seismic activity (e.g. Hayakawa et al. 2006, and associated special issue; Fraser-Smith 2008), particularly as precursors (Dovbyna 2007). Causative mechanisms are often discussed in terms of ionospheric perturbations, although there have also been many reports of no correlation between ULF/ELF/VLF phenomena, ionospheric properties and earthquakes (e.g. Rodger et al. 1996). It has also been suggested that the spectral power law across the ULF range is modified by the appearance of flicker noise before large seismic events (Smirnova and Hayakawa 2007).

Bortnik et al. (2008b) described a detailed and careful statistical study, spanning 7.5 years, of Pc1events (8913 events) and nearby earthquakes (434 $M > 3.0$ events within 200 km) at a low latitude site. They found a statistically significant increase, by a factor of 3–5, in the occurrence probability of daytime Pc1 pulsations ~5–15 days prior to an earthquake. Their results are summarized in Fig. 13.16. Evidence of earthquake precursors in the 0.01–0.5 Hz range has also been provided by Fraser-Smith et al. (1990) and Fraser-Smith (2008).

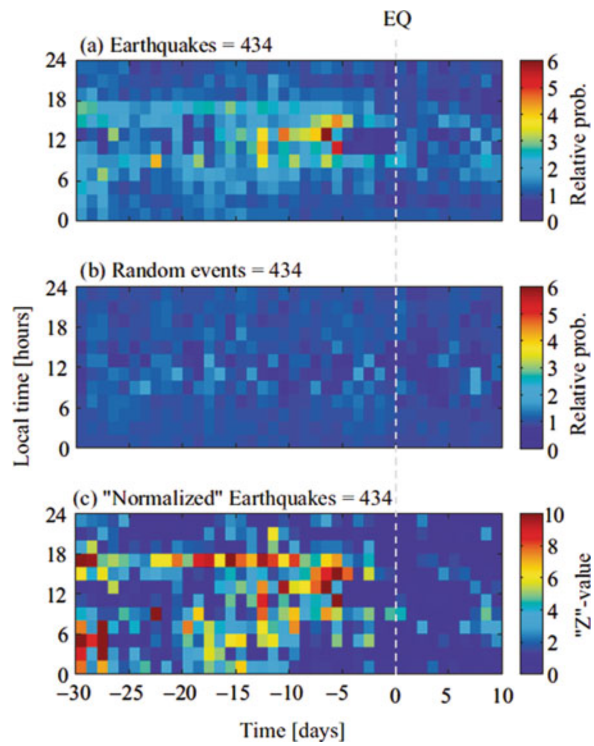

Fig. 13.16 Relative probability of Pc1 occurrence (**a**) prior to an earthquake, (**b**) with respect to a similar number of random events, and (**c**) normalized for LT. (Figure 4a–c from Bortnik et al. 2008b)

One of the main difficulties in this type of work is discriminating any seismic effect from the background of naturally-occurring global geomagnetic pulsations and artificial noise effects. Hattori et al. (2004a) examined for this purpose the effectiveness of a principal component analysis method, based on eigenvalue analysis of the covariance matrix of the observed signal matrix, for frequencies >10 mHz and $M > 6$ earthquakes. They also accounted for possible shaking of the sensors. Looking at 8 months data, they found earthquake-related enhancements in ULF activity first appeared about 2 weeks prior to and peaking a few days before, a large earthquake, with an average intensity of order 10^{-2} nT over the frequency range. Further extensive studies were reported in Hattori et al. (2004b, 2006). Fraser-Smith et al. (1990) reported similar effects, including 'an exceptionally high level of activity' immediately preceding an $M = 7.1$ earthquake.

There have also been recent reports that Pc1 pulsations present a potential hazard for myocardial infarction (Kleimenova et al. 2007) and other medical conditions (Matveyeva and Shchepetnov 2007). The former reports a study of nearly 86,000 instances over 3 years, suggesting that in winter, days of high myocardial incidence correspond with high Pc1 incidence.

There is much discussion in the media regarding human effects on the environment. Guglielmi and Zotov (2007) considered whether there may be a weekend effect of human origin on Pc1 wave occurrence. They examined Pc1 activity at Borok (L=2.9) over 1958–1992 and found an inherent enhancement in Pc1 occurrence of about 10% on weekends, and

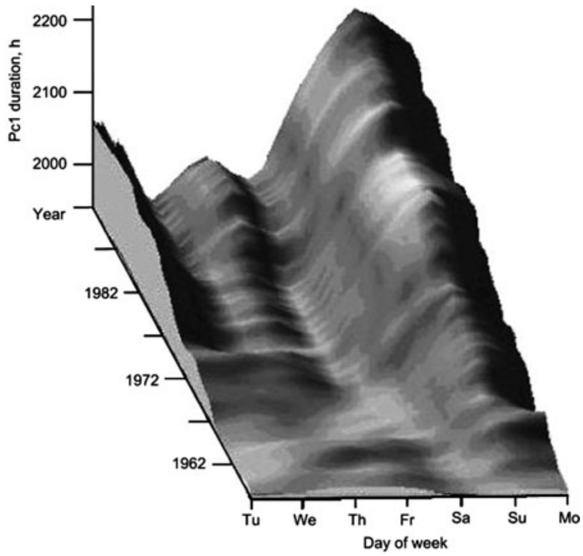

Fig. 13.17 Evolution of the weekend effect in Pc1 activity over 35 years (Figure 4 from Guglielmi and Zotov 2007)

that this value is increasing: see Fig. 13.17. In a previous 12-year study of Pc1 activity Fraser-Smith (1979) suggested that such an effect may be related to the level of power line harmonic radiation into the magnetosphere during weekends. This is an outstanding question: for example, could lower levels of artificial noise on weekends simply facilitate detection?

In conclusion, further work is required to establish whether enhanced Pc1 activity may generally precede earthquakes, and if so, the physical mechanism. The cause of the weekend effect in Pc1 activity also needs to be established.

References

Abe S, Kawano H, Goldstein J, Ohtani S, Solovyev SI, Baishev DG, Yumoto K (2006) Simultaneous identification of a plasmaspheric plume by a ground magnetometer pair and IMAGE Extreme Ultraviolet Imager. J Geophys Res. doi:10.1029/2006JA011653

Ables ST, Fraser BJ (2005) Observing the open-closed boundary using cusp-latitude magnetometers. Geophys Res Lett. doi:10.1029/2005GL022824

Albert JM, Bortnik J (2009) Nonlinear interaction of radiation belt electrons with electromagnetic ion cyclotron waves. Geophys Res Lett. doi:10.1029/2009GL038904

Allan W, Poulter EM (1984) The spatial structure of different ULF pulsation types: a review of STARE radar results. Rev Geophys 22:85–97

Allan W, Poulter EM (1992) ULF waves – their relationship to the structure of the Earth's magnetosphere. Rep Prog Phys 55:533–598

Allan W, White SP, Poulter EM (1986a) Impulse-excited hydromagnetic cavity and field-line resonances in the magnetosphere. Planet Space Sci 34:371–385

Allan W, White SP, Poulter EM (1986b) Hydromagnetic wave coupling in the magnetosphere – plasmapause effects on impulse-excited resonances. Planet Space Sci 34: 1189–1200

Altman C, Fijalkow E (1980) The horizontal propagation of Pc1 micropulsations in the ionosphere. Planet Space Sci 28:61–68

Andrews MK (1977) Magnetic pulsation behaviour in the magnetosphere inferred from whistler mode signals. Planet Space Sci 25:957–966

Archer M, Horbury TS, Lucek EA, Mazelle C, Balogh A, Dandouras I (2005) Size and shape of ULF waves in the terrestrial foreshock. J Geophys Res. doi:10.1029/2004JA010791

Arnoldy RL, Engebretson MJ, Alford JL, Erlandson RE, Anderson BJ (1996) Magnetic impulse events and associated Pc 1 bursts at dayside high latitudes. J Geophys Res. doi:10.1029/95JA03378

Arnoldy RL et al (2005) Pc 1 waves and associated unstable distributions of magnetospheric protons observed during a solar wind pressure pulse. J Geophys Res. doi:10.1029/2005JA011041

Baddeley LJ, Yeoman TK, Wright DM, Trattner KJ, Kellet BJ (2005a) On the coupling between unstable magnetospheric particle populations and resonant high *m* ULF wave signatures in the ionosphere. Ann Geophys 23: 567–577

Baddeley LJ, Yeoman TK, Wright DM (2005b) HF Doppler sounder measurements of the ionospheric signatures of small scale ULF waves. Ann Geophys 23:1807–1820

Badman SV, Wright DM, Clausen LBN, Fear RC, Robinson TR, Yeoman TK (2009) Cluster spacecraft observations of a ULF wave enhanced by Space Plasma Exploration by Active Radar (SPEAR). Ann Geophys 27:3591–3599

Belyaev PP, Polyakov SV, Rapoport VO, Trakhtengerts VY (1989) Theory of formation of the resonance spectral structure of atmospheric electromagnetic noise background in the range of short-period geomagnetic pulsations. Izvestiya vuzov-Radiofizika 32:802–810

Berube D, Moldwin MB, Weygand JM (2003) An automated method for the detection of field line resonance frequencies using ground magnetometer techniques. J Geophys Res. doi:10.1029/2002JA009737

Berube D, Moldwin MB, SF Fung, Green JL (2005) A plasmaspheric mass density model and constraints on its heavy ion concentration. J Geophys Res. doi:10.1029/2004JA010684

Berube D, Moldwin MB, Ahn M (2006) Computing magnetospheric mass density from field line resonances in a realistic magnetic field geometry. J Geophys Res. doi:10.1029/2005JA011450

Blanco-Cano X, Omidi N, Russell CT (2009) Global hybrid simulations: foreshock waves and cavitons under radial interplanetary magnetic field geometry. J Geophys Res. doi:10.1029/2008JA013406

Blum LW, MacDonald EA, Gary SP, Thomsen MF, Spence HE (2009) Ion observations from geosynchronous orbit as a proxy for ion cyclotron wave growth during storm times. J Geophys Res. doi:10.1029/2009JA014396

Bortnik J, Cutler JW, Dunson C, Bleier TE (2007) An automatic wave detection algorithm applied to Pc1 pulsations. J Geophys Res. doi:10.1029/2006JA011900

Bortnik J, Cutler JW, Dunson C, Bleier TE, McPherron RL (2008a) Characteristics of low-latitude Pc1 pulsations during geomagnetic storms. J Geophys Res. doi:10.1029/2007JA012867

Bortnik J, Cutler JW, Dunson C, Bleier TE (2008b) The possible statistical relation of Pc1 pulsations to Earthquake occurrence at low latitudes. Ann Geophys 26:2825–2836

Bösinger T, Haldoupis C, Belyaev PP, Yakunin MN, Semenova NV, Demekhov AD, Angelopolous V (2002) Spectral properties of the ionospheric Alfvén resonator observed at a low-latitude station ($L = 1.3$). J Geophys Res. doi:10.1029/2001JA005076

Bösinger T, Ermakova EN, Haldoupis C, Kotik DS (2009) Magnetic-inclination effects in the spectral resonance structure of the ionospheric Alfvén resonator. Ann Geophys 27:1313–1320

Boudouridis A, Zesta E (2007) Comparison of Fourier and wavelet techniques in the determination of geomagnetic field line resonances. J Geophys Res. doi:10.1029/2006JA011922

Brautigam DH, Ginet GP, Albert JM, Wygant JR, Rowland DE, Ling A, Bass J (2005) CRRES electric field power spectra and radial diffusion coefficients. J Geophys Res. doi:10.1029/2004JA010612

Broughton MC, Engebretson MJ, Glassmeier K-H, Narita Y, Keiling A, Fornaçon K-H, Parks GK, Remè H (2008) Ultra-low-frequency waves and associated wave vectors observed in the plasma sheet boundary layer by Cluster. J Geophys Res. doi:10.1029/2008JA013366

Chaston CC, Peticolas LM, Bonnell JW, Carlson CW, Ergun RE, McFadden JP, Strangeway RJ (2003) Width and brightness of auroral arcs driven by inertial Alfven waves. J Geophys Res. doi:10.1029/2001JA007537

Chen L, Thorne RM, Horne RB (2009) Simulation of EMIC wave excitation in a model magnetosphere including structured high-density plumes. J Geophys Res. doi:10.1029/2009JA014204

Chi PJ, Russell CT (2005) Travel-time magnetoseismology: Magnetospheric sounding by timing the tremors in space. Geophys Res Lett. doi:10.1029/2005GL023441

Chi PJ, Russell CT (2008) Use of the Wigner-Ville distribution in interpreting and identifying ULF waves in triaxial magnetic records. J Geophys Res. doi:10.1029/2007JA012469

Chi P et al (2001)Propagation of the preliminary reverse impulse of sudden commencements to low latitudes. J Geophys Res 106:18857–18864

Chi PJ, Lee DH, Russell CT (2006) Tamao travel time of sudden impulses and its relationship to ionospheric convection vortices. J Geophys Res. doi:10.1029/2005JA011578

Chisham G, Orr D, Taylor MJ, Lühr H (1990) The magnetic and optical signature of a Pg pulsation. Planet Space Sci 38:1443–1456

Chisham G et al (2007) A decade of the Super Dual Auroral Radar Network (SuperDARN): scientific achievements, new techniques and future directions. Surv Geophys. doi:10.1007/s10712-007-9017-8

Claudepierre SG, Elkington SR, Wiltberger M (2008) Solar wind driving of magnetospheric ULF waves: pulsations driven by velocity shear at the magnetopause. J Geophys Res. doi:10.1029/2007JA012890

Clausen LBN, Yeoman TK (2009) Comprehensive survey of Pc4 and Pc5 band spectral content in cluster magnetic field data. Ann Geophys 27:3237–3248

Clausen LBN, Yeoman TK, Wright DM, Robinson TR, Dhillon RS, Gane SC (2008) First results of a ULF wave injected on open field lines by Space Plasma Exploration by Active Radar (SPEAR). J Geophys Res. doi:10.1029/2007JA012617

Clausen LBN, Yeoman TK, Fear RC, Behlke R, Lucek EA, Engebretson MJ (2009) First simultaneous measurements of waves generated at the bow shock in the solar wind, the magnetosphere and on the ground. Ann Geophys 27:357–371

Clilverd MA, Smith AJ, Thomson NR (1991) The annual variation in quiet time plasmaspheric electron density, determined from whistler mode group delays. Planet Space Sci 39:1059–1067

Clilverd MA et al (2003) In situ and ground-based intercalibration measurements of plasma density at $L = 2.5$. J Geophys Res. doi:10.1029/2003JA009866

Clilverd MA, Meredith NP, Horne RB, Glauert SA, Anderson RR, Thomson NR, Menk FW, Sandel BR (2007a) Longitudinal and seasonal variations in plasmaspheric electron density: implications for electron precipitation. J Geophys Res. doi:10.1029/2007JA012416

Clilverd MA, Rodger CJ, Millan RM, Sample JG, Kokorowski M, McCarthy MP, Ulich T, Raita T, Kavanagh AJ, Spanswick E (2007b) Energetic particle precipitation into the middle atmosphere triggered by a coronal mass ejection. J Geophys Res. doi:10.1029/2007JA012395

Constantinescu OD, Glassmeier K-H, Décréau PME, Fränz M, Fornaçon K-H (2007) Low frequency wave sources in the outer magnetosphere, magnetosheath, and near Earth solar wind. Ann Geophys 25:2217–2228

Constantinescu OD et al (2009) THEMIS observations of duskside compressional Pc5 waves. J Geophys Res. doi:10.1029/2008JA013519

Cornwall JM (1965) Cyclotron instabilities and electromagnetic emissions in the ultra low frequency and very low frequency ranges. J Geophys Res 70:61–69

Criswell D (1969) Pc 1 micropulsation activity and magnetospheric amplification of 0.2 to 5.0 Hz hydromagnetic waves. J Geophys Res 74:205–224

Cummings W, O'Sullivan R, Coleman P Jr (1969) Standing Alfvén waves in the magnetosphere. J Geophys Res 74:778–793

Degeling AW, Rankin R, Kabin K, Marchard R, Mann IR (2006) The effect of ULF compressional modes and field line resonances on relativistic electron dynamics. Planet Space Sci. doi:10.1016/j.pss.2006.04.039

Degeling AW, Ozeke LG, Rankin R, Mann IR, Kabin K (2008) Drift resonant generation of peaked relativistic electron distributions by Pc5 ULF waves. J Geophys Res. doi:10.1029/2007JA012411

Degeling AW, Rankin R, Kabin K, Rae IJ, Fenrich FR (2010) Modeling ULF waves in a compressed dipole magnetic field. J Geophys Res. doi:10.1029/2010JA015410

Demekhov AG (2007) Recent progress in understanding Pc1 pearl formation. J Atmos Sol Terr Phys 69:1609–1622

Demekhov AG, Belyaev PP, Isaev SV, Manninen J, Turunen T, Kangas J (2000) Modelling the diurnal evolution of the resonance spectral structure of the atmospheric noise background in the Pc1 frequency range. J Atmos Sol Terr Phys 62:257–265

Dent ZC, Mann IR, Menk FW, Goldstein J, Wilford CR, Clilverd MA, Ozeke LG (2003) A coordinated ground-based and IMAGE satellite study of quiet-time plasmaspheric density profiles. Geophys Res Lett. doi:10.1029/2003GL016946

Dent ZC, Mann IR, Goldstein J, Menk FW, Ozeke LG (2006) Plasmaspheric depletion, refilling, and plasmapause dynamics: a coordinated ground-based and IMAGE satellite study. J Geophys Res. doi:10.1029/2005JA011046

Denton R, Gallagher D (2000) Determining the mass density along magnetic field lines from toroidal eigenfrequencies. J Geophys Res 105:27717–27725

Denton RE et al. (2009) Field line distribution of density at L=4.8 inferred from observations by CLUSTER. Ann Geophys 27:705–724

Dovbyna BV (2007) On the earthquake effects in the regime of Pc1. J Atmos Sol Terr Phys 69:1765–1769

Dungey JW, Southwood DJ (1970) Ultra low frequency waves in the magnetosphere. Space Sci Rev. doi:10.1007/BF0017551

Dyrud L, Engebretson M, Posch J, Hughes W, Fukunishi H, Arnoldy R, Newell P, Horne R (1997) Ground observations and possible source regions of two types of Pc 1-2 micropulsations at very high latitudes. J Geophys Res 102:27011–27027

Dyrud LP, Behnke R, Kepko EL, Sulzer M, Zafke S (2008) Ionospheric ULF oscillations driven from above Arecibo. Geophys Res Lett. doi:10.1029/2008GL034073

Elkington SR (2006) A review of ULF interactions with radiation belt electrons. In: Takahashi K, Chi PJ, Denton RE, Lysak RL (eds) Magnetospheric ULF waves: synthesis and new directions. American Geophysical Union, Washington, DC, pp 177–193

Elkington SR, Hudson MK, Chan AA (2003) Resonant acceleration and diffusion of outer zone electrons in an asymmetric geomagnetic field. J Geophys Res. doi:10.1029/2001JA009202

Engebretson M, Zanetti L, Potemra T, Baumjohann W, Lühr H, Acuna M (1987) Simultaneous observations of Pc3-4 pulsations in the solar wind and in the Earth's magnetosphere. J Geophys Res. doi:10.1029/JA092iA09p10053

Engebretson MJ, Posch JL, Pilipenko VA, Chugunova OM (2006) ULF waves at very high latitudes. In: Takahashi K, Chi PJ, Denton RE, Lysak RL (eds) Magnetospheric ULF waves: synthesis and new directions. American Geophysical Union, Washington, DC, pp 137–156

Engebretson MJ et al (2007) Cluster observations of Pc1-2 waves and associated ion distributions during the October and November 2003 magnetic storms. Planet Space Sci 55:829–848

Engebretson MJ et al (2008a) Pc1-2 waves and energetic particle precipitation during and after magnetic storms: superposed epoch analysis and case studies. J Geophys Res. doi:10.1029/2007JA012362

Engebretson MJ, Posch JL, Westermann AM, Otto NJ, Slavin JA, Le G, Strangeway RJ, Lessard MR (2008b) Temporal and spatial characteristics of Pc1 waves observed by ST5. J Geophys Res. doi:10.1029/2008JA013145

Engebretson MJ, Moen J, Posch JL, Lu F, Lessard MC, Kim H, Lorentzen DA (2009) Searching for ULF signatures of the cusp: observations from search coil magnetometers and auroral imagers in Svalbard. J Geophys Res. doi:10.1029/2009JA014287

Eriksson PTI, Blomberg LG, Walker ADM, Glassmeier K-H (2005) Poloidal ULF oscillations in the dayside magnetosphere: a cluster study. Ann Geophys 23:2679–2686

Eriksson PTI, Blomberg LG, Glassmeier K-H (2006a) Cluster satellite observations of mHz pulsations in the dayside magnetosphere. Adv Space Res 38:1730–1737

Eriksson PTI, Walker ADM, Stephenson JAE (2006b) A statistical correlation of Pc5 pulsations and solar wind pressure oscillations. Adv Space Res 38:1763–1771

Erikkson PTI, Blomberg LG, Schaefer S, Glassmeier K-H (2008) Sunward propagating Pc5 waves observed on the post-midnight magnetospheric flank. Ann Geophys 26:1567–1579

Erlandson RE, Anderson BJ (1996) Pc 1 waves in the ionosphere: a statistical study. J Geophys Res 101:7843–7857

Erlandson RE, Mursula K, Bösinger T (1996) Simultaneous ground-satellite observations of structured Pc 1 pulsations. J Geophys Res 101:27149–27156

Fenrich FR, Waters CL (2008) Phase coherence analysis of a field line resonance and solar wind oscillation. Geophys Res Lett. doi:10.1029/2008GL035430

Feygin FZ, Nekrasov AK, Pikkarainen T, Raita T, Prikner K (2007) Pc1 pearl waves with magnetosonic dispersion. J Atmos Sol Terr Phys 69:1644–1650

Francia P, Villante U (1997) Some evidence of ground power enhancements at frequencies of global magnetospheric modes at low latitude. Ann Geophys 15:17–23

Francia P, De Laurentis M, Vellante M, Paincatelli A (2009) ULF geomagnetic pulsations at different latitudes in Antarctica. Ann Geophys 27:3621–3629

Fraser BJ (1982) Pc1-2 observations of heavy ion effects by synchronous satellite ATS-6. Planet Space Sci 30:1229–1238

Fraser BJ (2007) ULF waves: exploring the Earth's magnetosphere. In: Duldig M (ed) Advances in geosciences, vol 14. Solar Terrestrial, World Scientific, Singapore, pp 1–32

Fraser BJ, McPherron RL (1982) Pc 1-2 magnetic pulsation spectra and heavy ion effects at synchronous orbit: ATS 6 results. J Geophys Res 87:4560–4566

Fraser BJ, Singer HJ, Hughes WJ, Wygant JR, Anderson RR, Hu YD (1996) CRRES Poynting vector observations of electromagnetic ion cyclotron waves near the plasmapause. J Geophys Res 101:15331–15343

Fraser BJ, Horwitz JL, Slavin JA, Dent ZC, Mann IR (2005) Heavy ion mass loading of the geomagnetic field near the plasmapause and ULF wave implications. Geophys Res Lett. doi:10.1029/2004GL021315

Fraser-Smith AC (1979) A weekend increase in geomagnetic activity. J Geophys Res 84:2089–2096

Fraser-Smith AC (2008) Ultralow-frequency magnetic fields preceding large earthquakes. Eos Trans AGU. doi:10.1029/2008EO230007

Fraser-Smith AC, Bernardi A, McGill PR, Ladd ME, Helliwell RA, Villard OG Jr (1990) Low-frequency magnetic field measurements near the epicenter of the Ms 7.1 Loma Prieta earthquake. Geophys Res Lett 17:1465–1468

Frey HU, Haerendel G, Mende SB, Forrester WT, Immel TJ, Østgaard N (2004) Subauroral morning proton spots (SAMPS) as a result of plasmapause-ring current interaction. J Geophys Res. doi:10.1029/2004JA010516

Fuselier SA, Gary SP, Thomsen MF, Claflin ES, Hubert B, Sandel BR, Immel T (2004) Generation of transient dayside subauroral proton precipitation. J Geophys Res. doi:10.1029/2004JA010393

Gamayunov KV, Khazanov GV (2008) Crucial role of ring current H+ in electromagnetic ion cyclotron wave dispersion relation: results from global simulations. J Geophys Res. doi:10.1029/2008JA013494

Gamayunov KV, Khazanov GV, Liemohn MW, Fok MC, Ridley AJ (2009) Self-consistent model of magnetospheric electric field, ring current, plasmasphere, and electromagnetic ion cyclotron waves: Initial results. J Geophys Res. doi:10.1029/2008JA013597

Ganguly S, Behnke R (1982) Short-period fluctuations in F region ionization observed at Arecibo. J Geophys Res 87:261–264

Gjerloev JW et al (2007) Observations of Pi2 pulsations by the Wallops HF radar in association with substorm expansion. Geophys Res Lett. doi:10.1029/2007GL030492

Gomberoff L (2008) Electrostatic instabilities triggered by finite amplitude Alfvén/ion-cyclotron waves and relative drifts among the ion components in the magnetosphere. J Geophys Res. doi:10.1029/2008JA013378

Greenstadt EW, Mellott MM, McPherron RL, Russell CT, Singer HJ, Knecht DJ (1983) Transfer of pulsation-related wave activity across the magnetopause: observations of corresponding spectra by ISEE1 and ISEE2. Geophys Res Lett 10:659–662

Greenwald RA, Walker ADM (1980) Energetics of long period resonant hydromagnetic waves. Geophys Res Lett 7:745–748

Grew RS, Menk FW, Clilverd MA, Sandel BR (2007) Mass and electron densities in the inner magnetosphere during a prolonged disturbed interval. Geophys Res Lett. doi:10.1029/2006GL028254

Guglielmi A, Zotov O (2007) The human impact on Pc1 wave activity. J Atmos Sol Terr Phys 69:1753–1758

Gul'yel'mi AV (1966) Plasma concentration at great heights according to data on toroidal fluctuations of the magnetosphere. Geomagn Aeron 6:98

Hansen HJ, Fraser BJ, Menk FW, Hu Y-D, Newell PT, Meng C-I, Morris RJ (1992) High-latitude Pc1 bursts arising in the dayside boundary layer region. J Geophys Res 97: 3993–4008

Hansen HJ, Fraser BJ, Menk FW, Erlandson RR (1995) Ground-satellite observations of Pc-1 magnetic pulsations in the plasma trough. J Geophys Res 100:7971–7985

Hasegawa H et al (2009) Kelvin-Helmholtz waves at the Earth's magnetopause: multiscale development and associated reconnection. J Geophys Res. doi:10.1029/2009JA014042

Hattingh SKF, Sutcliffe PR (1987) Pc3 pulsation eigenperiod determination at low latitudes. J Geophys Res 92:12433–12436

Hattori K, Serita A, Gotoh K, Yoshino C, Harada M, Isezaki N, Hayakawa M (2004a) ULF geomagnetic activity associated with the 2000 Izu Islands earthquake swarm. Jpn Phys Chem Earth 29:425–435

Hattori K et al (2004b) ULF geomagnetic field measurements in Japan and some recent results associated with Iwateken Nairiku Hokubu earthquakes in 1998. Phys Chem Earth 29:481–494

Hattori K, Serita A, Yoshino C, Hayakawa M, Isezaki N (2006) Singular spectral analysis and principal component analysis for signal discrimination of ULF geomagnetic data associated wth 2000 Izu Island Earthquake Swarm. Phys Chem Earth 31:281–291

Hayakawa M, Pulinets S, Parrot M, Molchanov O (2006) Recent progress in seismo-electromagnetic and related phenomena. Phys Chem Earth 31:129–131

Hebden SR, Robinson TR, Wright DM, Yeoman T, Raita T, Bösinger T (2005) A quantitative analysis of the diurnal evolution of the Ionosphere Alfvén resonator magnetic resonance features and calculation of changing IAR parameters. Ann Geophys 23:1711–1721

Heilig B, Lühr H, Rother M (2007) Comprehensive study of ULF upstream waves observed in the topside ionosphere by CHAMP and on the ground. Ann Geophys 25: 737–754

Heilig B, Lotz S, Verö J, Sutcliffe P, Reda J, Pajunpää K, Raita T (2010) Empirically modelled Pc3 activity based on solar wind parameters. Ann Geophys 28:1703–1722

Horita RE, Barfield JN, Heacock RR, Kangas J (1979) IPDP source regions and resonant proton energies. J Atmos Sol Terr Phys 41:293–309

Horne RB et al (2005) Wave acceleration of electrons in the Van Allen radiation belts. Nature. doi:10.1038/nature03939

Horne RB, Thorne RM, Glauert SA, Meredith NP, Pokhotelov D, Santolik O (2007) Electron acceleration in the Van Allen radiation belts by fast magnetosonic waves. Geophys Res Lett. doi:10.1029/2007GL030267

Howard TA, Menk FW (2001) Propagation of 10–50 mHz ULF waves with high spatial coherence at high latitudes. Geophys Res Lett 28:231–234

Howard TA, Menk FW (2005) Ground observations of high-latitude Pc3-4 ULF waves. J Geophys Res. doi:10.1029/2004JA010417

Hughes WJ (1974) The effect of the atmosphere and ionosphere on long period magnetospheric micropulsations. Planet Space Sci 22:1157–1172

Hughes WJ (1983) Hydromagnetic waves in the magnetosphere. In: Carovillano RL, Forbes JM (eds) Solar-terrestrial physics. Reidel D, Dordrecht, pp 453–477

Hughes W, McPherron R, Barfield J (1978) Geomagnetic pulsations observed simultaneously on three geostationary satellites. J Geophys Res 83:1109–1116

Jacobs JA, Watanabe T (1964) Micropulsation whistlers. J Atmos Sol Terr Phys 26:825–829

Jordanova VK, Spasojević M, Thomsen MF (2007) Modeling the electromagnetic ion cyclotron wave-induced formation of detached subauroral proton arcs. J Geophys Res. doi:10.1029/2006JA012215

Jordanova VK, Albert J, Miyoshi Y (2008) Relativistic electron precipitation by EMIC waves from self-consistent global simulations. J Geophys Res. doi:10.1029/2008JA013239

Kabin K, Rankin R, Mann IR, Degeling AW, Marchand R (2007) Polarization properties of standing shear Alfvén waves in non-axisymmetric background magnetic fields. Ann Geophys 25:815–822

Kale ZC, Mann IR, Waters CL, Goldstein J, Menk FW, Ozeke LG (2007) Ground magnetometer observation of a cross-phase reversal at a steep plasmapause. J Geophys Res. doi:10.1029/2007JA012367

Kale ZC, Mann IR, Waters CL, Vellante M, Zhang TL, Honary F (2009) Plasmaspheric dynamics resulting from the Hallowe'en 2003 geomagnetic storm. J Geophys Res. doi:10.1029/2009JA014194

Karatay S, Arikan F, Arikan O (2010) Investigation of total electron content variability due to seismic and geomagnetic disturbances in the ionosphere. Radio Sci. doi:10.1029/2009RS004313

Kataoka R, Miyoshi Y, Morioka A (2009) Hilbert-Huang transform of geomagnetic pulsations at auroral expansion onset. J Geophys Res. doi:10.1029/2009JA014214

Keiling A, Parks GK, Wygant JR, Dombeck J, Mozer FS, Russell CT, Streltsov AV, Lotko W (2005) Some properties of Alfvén waves: observations in the tail lobes and the plasma sheet boundary layer. J Geophys Res. doi:10.1029/2004JA010907

Kepko L, Spence HE (2003) Observations of discrete, global magnetospheric oscillations directly driven by solar wind velocity variations. J Geophys Res. doi:10.1029/2002JA009676

Kessel RL (2008) Solar wind excitation of Pc5 fluctuations in the magnetosphere and on the ground. J Geophys Res. doi:10.1029/2007JA012255

Kessel RL, Mann IR, Fung SF, Milling DK, O'Connell N (2004) Correlation of Pc5 wave power inside and outside the magnetosphere during high speed streams. Ann Geophys 21:629–641

Khazanov GV, Gamayunov KV (2007) Effect of electromagnetic ion cyclotron wave normal angle distribution on relativistic electron scattering in the outer radiation belt. J Geophys Res. doi:10.1029/2007JA012282

Kim K-H, Lee DH, Takahashi K, Russell CT, Moon YJ, Yumoto K (2005) Pi2 pulsations observed from the Polar satellite outside the plasmapause. Geophys Res Lett. doi:10.1029/2005GL023872

Kivelson MG (2006) ULF waves from the ionosphere to the outer planets. In: Takahashi K, Chi PJ, Denton RE, Lysak RL (eds) Magnetospheric ULF waves: synthesis and new directions. American Geophysical Union, Washington, DC, pp 11–30

Kivelson MG, Southwood DJ (1985) Resonant ULF waves: a new interpretation. Geophys Res Lett 12:49–52

Kivelson MG, Southwood DJ (1986) Coupling of global magnetospheric MHD eigenmodes to field line resonances. Geophys Res Lett 91:4345–4351

Kleimenova NG, Kozyreva OV, Breus TK, Rapoport SI (2007) Pc1 geomagnetic pulsations as a potential hazard of the myocardial infarction. J Atmos Sol Terr Phys 69: 1759–1764

Klimushkin D (1998) Resonators for hydromagnetic waves in the magnetosphere. J Geophys Res 103:2369–2375

Korotova GI, Sibeck DG, Kondratovich V, Angelopolous V, Constantinescu OD (2009) THEMIS observations of compressional pulsations in the dawn-side magnetosphere: a case study. Ann Geophys 27:3725–3735

Kozlov DA, Leonovich AS (2008) The structure of field line resonances in a dipole magnetosphere with moving plasma. Ann Geophys 26:689–698

Krauss-Varban D (1994) Bow shock and magnetosheath simulations: wave transport and kinetic properties. In: Engebretson MJ, Takahashi K, Scholer M (eds) Solar wind sources of magnetospheric Ultra-Low Frequency waves. American Geophysical Union, Washington, DC, pp 121–134

Kurazhkovskaya NA, Klain BI, Dovbyna BV (2007) Patterns of simultaneous observations of high-latitude magnetic impulses (MIEs) and impulsive bursts in the Pc1-2 band. J Atmos Sol Terr Phys 69:1680–1689

Le G, Russell CT (1996) Solar wind control of upstream wave frequency. J Geophys Res 101:2571–2575

Lee DH, Lysak R (1999) MHD waves in a three-dimensional dipolar magnetic field: a search for Pi2 pulsations. J Geophys Res 104:28691–28699

Lee D-H, Takahashi K (2006) MHD eigenmodes in the inner magnetosphere. In: Takahashi K, Chi PJ, Denton RE, Lysak RL (eds) Magnetospheric ULF waves: synthesis and new directions. American Geophysical Union, Washington, DC, pp 73–90

Lee EA, Mann IR, Loto'aniu, TM, Dent ZC (2007)Global Pc5 pulsations observed at unusually low L during the great magnetic storm of 24 March 1991. J Geophys Res. doi:10.1029/2006JA011872

Lee D-H, Johnson JR, Kim K, Kim K-S (2008) Effects of heavy ions on ULF wave resonances near the equatorial region. J Geophys Res. doi:10.1029/2008JA013088

Liou K, Takahashi K, Newell PT, Yumoto K (2008) Polar Ultraviolet Imager observations of solar wind-driven ULF auroral pulsations. Geophys Res Lett. doi:10.1029/2008GL034953

Liu YH, Fraser BJ, Ables ST, Dunlop MW, Zhang BC, Liu RY, Zong QG (2008) Phase structure of Pc3 waves observed by Cluster and ground stations near the cusp. J Geophys Res. doi:10.1029/2007JA012754

Liu W, Sarris TE, Li X, Elkington SR, Ergun R, Angelopolous V, Bonnell J, Glassmeier KH (2009a) Electric and magnetic field observations of Pc4 and Pc5 pulsations in the inner magnetosphere: a statistical study. J Geophys Res. doi:10.1029/2009JA014243

Liu YH, Fraser BJ, Ables ST, Zhang BC, Liu RY, Dunlop MW, Waterman J (2009b) Transverse scale size of Pc3 ULF waves near the exterior cusp. J Geophys Res. doi:10.1029/2008JA013971

Lorentzen KR, McCarthy MP, Parks GK, Foat JE, Millan RM, Smith DM, Lin RP, Treilhou JP (2000) Precipitation of relativistic electrons by interaction with electromagnetic ion cyclotron waves. J Geophys Res 105:5381–5389

Loto'aniu TM, Waters CL, Fraser BJ, Samson JC (1999) Plasma mass density in the plasmatrough: comparison using ULF waves and CRRES. Geophys Res Lett 26:3277–3280

Loto'aniu TM, Fraser BJ, Waters CL (2005) The propagation of electromagnetic ion cyclotron wave energy in the magnetosphere. J Geophys Res. doi:10.1029/2004JA010816

Loto'aniu TM, Thorne RM, Fraser BJ, Summers D (2006) Estimating relativistic electron pitch angle scattering rates using properties of the electromagnetic ion cyclotron wave spectrum. J Geophys Res. doi:10.1029/2005JA011452

Loto'aniu TM, Fraser BJ, Waters CL (2009) The modulation of electromagnetic ion cyclotron waves by Pc5 ULF waves. Ann Geophys 27:121–130

Lu JY, Rankin R, Marchand R, Rae IJ, Wang W, Solomon SC, Lei J (2007) Electrodynamics of magnetosphere-ionosphere coupling and feedback on magnetospheric field line resonances. J Geophys Res. doi:10.1029/2006JA012195

Lysak RL, Song Y (2008) Propagation of kinetic Alfvén waves in the ionospheric Alfvén resonator in the presence of density cavities. Geophys Res Lett. doi:10.1029/2008GL035728

Maeda N et al (2008) Simultaneous observations of the plasma density on the same field line by the CPMN ground magnetometers and the cluster satellites. Adv Space Res. doi:10.1016/j.asr.2008.04.016

Manchester RN (1970) Propagation of hydromagnetic emissions in the ionospheric duct. Planet Space Sci 18:299–307

Mann IR, Wright AN, Mills KJ, Nakariakov VM (1999) Excitation of magnetospheric waveguide modes by magnetosheath flows. J Geophys Res 104:333–353

Mann IR, O'Brien TP, Milling DK (2004) Correlations between ULF wave power, solar wind speed, and relativistic electron flux in the magnetosphere: solar cycle dependence. J Atmos Solar-Terr Phys. doi:10.1016/j.jastp.2003.10.002

Mathie RA, Mann IR (2001) On the solar wind control of Pc5 ULF pulsation power at mid-latitudes: Implications for MeV electron acceleration in the outer radiation belt. J Geophys Res. doi:10.1029/2001JA000002

Mathie RA, Mann IR, Menk FW, Orr D (1996) Pc5 ULF pulsations associated with waveguide modes observed with the IMAGE magnetometer array. J Geophys Res 104: 7025–7036

Matsuoka H, Takahashi K, Kokubun S, Yumoto K, Yamamoto T, Solovyev SI, Vershinin EF (1997) Phase and amplitude structure of Pc 3 magnetic pulsations as determined from multipoint observations. J Geophys Res 102:2391–2403

Matveyeva ET, Shchepetnov RV (2007) Temporal characteristics and medical aspects of Pc1 geomagnetic pulsations. J Atmos Sol Terr Phys 69:1747–1752

McCollough JP, Elkington SR, Baker DN (2009) Modeling EMIC wave growth during the compression event of 29 June 2007. Geophys Res Lett. doi:10.1029/2009GL039985

Menk FW (1992) Characterization of ionospheric Doppler oscillations in the Pc3-4 and Pi2 magnetic pulsation frequency range. Planet Space Sci 40:495–507

Menk FW, Cole KD, Devlin JD (1983) Associated geomagnetic and ionospheric variations. Planet Space Sci 31:569–572

Menk FW, Fraser BJ, Hansen HJ, Newell PT, Meng C-I, Morris RJ (1992) Identification of the magnetospheric cusp and cleft using Pc1-2 ULF pulsations. J Atmos Sol Terr Phys 54:1021–1042

Menk FW, Fraser BJ, Hansen HJ, Newell PT, Meng C-I, Morris RJ (1993) Multistation observations of Pc1-2 ULF pulsations in the vicinity of the polar cusp. J Geomagnetism Geoelectricity 45:1159–1173

Menk FW, Marshall RA, Waters CL, Dunlop IS, Fraser BJ (1995) Geomagnetic pulsations in the ionosphere. Adv Space Res 16:121–129

Menk FW, Orr D, Clilverd MA, Smith AJ, Waters CL, Milling DK, Fraser BJ (1999) Monitoring spatial and temporal variations in the dayside plasmasphere using geomagnetic field line resonances. J Geophys Res. doi:10.1029/1999JA900205

Menk FW, Waters CL, Fraser BJ (2000) Field line resonances and waveguide modes at low latitudes. J Geophys Res. doi:10.1029/1999JA900268

Menk FW, Yeoman TK, Wright DM, Lester M, Honary F (2003) High-latitude observations of impulse-driven ULF pulsations in the ionosphere and on the ground. Ann Geophys 21:559–576

Menk FW, Mann IR, Smith AJ, Waters CL, Clilverd MA, Milling DK (2004) Monitoring the plasmapause using geomagnetic field line resonances. J Geophys Res. doi:10.1029/2003JA010097

Menk FW, Clilverd MA, Yearby KH, Milinevski G, Thomson NR, Rose MC (2006) ULF Doppler oscillations of $L = 2.5$ flux tubes. J Geophys Res. doi:10.1029/2005JA011192

Menk FW, Waters CL, Dunlop IS (2007) ULF Doppler oscillations in the low latitude ionosphere. Geophys Res Lett. doi:10.1029/2007GL029300

Meredith NP, Thorne RM, Horne RB, Summers D, Fraser BJ, Anderson RR (2003) Statistical analysis of relativistic electron energies for cyclotron resonance with EMIC waves observed on CRRES. J Geophys Res. doi:10.1029/2002JA009700

Mier-Jedrzejowicz WAC, Southwood DJ (1979) The east-west phase structure of mid-latitude geomagnetic pulsations in the 8–25 mHz band. Planet Space Sci 27:617–630

Millan RM, Thorne RM (2007) Review of radiation belt relativistic electron losses. J Atmos Sol Terr Phys. doi:10.1016/j.jastp.2006.06.019

Milling DK, Mann IR, Menk FW (2001) Diagnosing the plasmapause with a network of closely spaced ground-based magnetometers. Geophys Res Lett 28:115–118

Milling DK, Rae J, Mann IR, Murphy KR, Kale A, Russell CT, Angelopolous V, Mende S (2008) Ionospheric localization and expansion of long-period Pi1 pulsations at substorm onset. Geophys Res Lett. doi:10.1029/2008GL033672

Miyoshi Y, Sakaguchi K, Shiokawa K, Evans D, Albert J, Connors M, Jordanova V (2008) Precipitation of radiation belt electrons by EMIC waves, observed from ground and space. Geophys Res Lett. doi:10.1029/2008GL035727

Morley SK, Ables ST, Sciffer MD, Fraser BJ (2009) Multipoint observations of Pc1-2 waves in the afternoon sector. J Geophys Res. doi:10.1029/JA014162

Moser, T-J (1991) Shortest path calculation of seismic rays. Geophysics 56:59–67

Mthembu SH, Malinga SB, Walker ADM, Magnus L (2009) Characterization of ultra low frequency (ULF) pulsations and the investigation of their possible source. Ann Geophys 27:3287–3296

Murphy KR, Rae IJ, Mann IR, Milling DK, Watt CEJ, Ozeke L, Frey HU, Angelopoulos V, Russell CT (2009) Wavelet-based ULF wave diagnosis of substorm expansion phase onset. J Geophys Res. doi:10.1029/2008JA013548

Mursala K (2007) Satellite observations of Pc1 pearl waves: the changing paradigm. J Atmos Sol Terr Phys 69:1623–1634

Mursula K, Rasinkangas R, Bösinger T, Erlandson R, Lindqvist PA (1997) Non-bouncing Pc 1 wave bursts. J Geophys Res 102:17611–17624

Ndiitwani DC, Sutcliffe PR (2009) The structure of low-latitude Pc3 pulsations observed by CHAMP and on the ground. Ann Geophys 27:1267–1277

Ndiitwani DC, Sutcliffe PR (2010) A study of L-dependent Pc3 pulsations observed by low Earth orbiting CHAMP satellite. Ann Geophys 28:407–414

Nishida A (1964) Ionospheric screening effect and storm sudden commencement. J Geophys Res 69:1861–1874

Nosé M, Iyemori T, Takeda M, Kamei T, Milling DK, Orr D, Singer HJ, Worthington EW, Sumitomo N (1998) Automated detection of Pi2 pulsations using wavelet analysis: 1. Method and an application for substorm monitoring. Earth Planets Space 50:773–783

Obana Y, Menk FW, Sciffer MD, Waters CL (2008) Quarter-wave modes of standing Alfvén waves detected by crossphase analysis. J Geophys Res. doi:10.1029/2007JA012917

Obana Y, Menk FW, Yoshikawa I (2010) Plasma refilling rates for $L = 2.3$–3.8 flux tubes. J Geophys Res. doi:10.1029/2009JA014191

Obayashi T (1965) Hydromagnetic whistlers. J Geophys Res 70:1069–1078

Obayashi T, Jacobs JA (1958) Geomagnetic pulsations and the Earth's outer atmosphere. Geophys J R Astron Soc 1: 53–63

O′Brien T, McPherron R, Sornette D, Reeves G, Friedel R, Singer H (2001) Which magnetic storms produce relativistic electrons at geosynchronous orbit? J Geophys Res 106:15533–15544

O'Brien TP et al (2003) Energization of relativistic electrons in the presence of ULF power and MeV microbursts: Evidence for dual ULF and VLF acceleration. J Geophys Res. doi:10.1029/2002JA009784

Odera TJ (1986) Solar wind controlled pulsations: a review. Rev Geophys. doi:10.1029/RG024i001p00055

Odera TJ, Van Swol D, Russell CT, Green CA (1991) Pc 3,4 magnetic pulsations observed simultaneously in the magnetosphere and at multiple ground stations. Geophys Res Lett 18:1671–1674

Olson JV, Lee LC (1983) Pc1 wave generation by sudden impulses. Planet Space Sci 31:295–302

Orr D (1984) Magnetospheric hydromagnetic waves: their eigenperiods, amplitudes and phase variations; a tutorial introduction. J Geophys 55:76–84

Ozeke LG, Mann IR (2008) Energization of radiation belt electrons by ring current ion driven ULF waves. J Geophys Res. doi:10.1029/2007JA012468

Ozeke LG, Mann IR, Rae IJ (2009) Mapping guided Alfvén wave magnetic field amplitudes observed on the ground to equatorial electric field amplitudes in space. J Geophys Res. doi:10.1029/2008JA013041

Pahud DM, Rae IJ, Mann IR, Murphy KR, Amalraj V (2009) Ground-based Pc5 ULF wave power: solar wind speed and MLT dependence. J Atmos Sol Terr Phys 71:1082–1092. doi:10.1016/jastp.2006.12.004

Pilipenko V, Federov E, Heilig B, Engebretson MJ (2008) Structure of ULF Pc3 waves at low altitudes. J Geophys Res. doi:10.1029/2008JA013243

Plaschke F, Glassmeier K-H, Auster HU, Constantinescu OD, Magnes W, Angelopolous V, Sibeck DG, McFadden JP (2008) Statistical analysis of ground based magnetic field measurements with the field line resonance detector. Ann Geophys 26:3477–3489

Plaschke P, Glassmeier KH, Auster HU, Constantinescu OD, Magnes W, Angelopoulos V, Sibeck DG, McFadden JP (2009a) Standing Alfvén waves at the magnetopause. Geophys Res Lett. doi:10.1029/2008GL036411

Plaschke F, Glassmeier K-H, Sibeck DG, Auster HU, Constantinescu OD, Angelopolous V, Magnes W (2009b) Magnetopause surface oscillation frequencies at different solar wind conditions. Ann Geophys 27:4521–4532

Ponomarenko PV, Menk FW, Waters CL (2003) Visualization of ULF waves in SuperDARN data. Geophys Res Lett. doi:10.1029/2003GL017757

Ponomarenko PV, Menk FW, Waters CL, Sciffer MD (2005) Pc3-4 ULF waves observed by the SuperDARN TIGER radar. Ann Geophys 23:1271–1280

Poole AWV, Sutcliffe PR (1987) Mechanisms for observed total electron content pulsations at mid latitudes. J Atmos Sol Terr Phys 49:231–236

Poole AWV, Sutcliffe PR, Walker ADM (1988) The relationship between ULF geomagnetic pulsations and ionospheric Doppler oscillations: derivation of a model. J Geophys Res 93:14656–14664

Potemra TA, Lühr H, Zanetti LJ, Takahashi K, Erlandson RE, Marklund GT, Block LP, Blomberg LG, Lepping RP (1989) Multisatellite and ground-based observations of transient ULF waves. J Geophys Res 94:2543–2554

Poulter E, Nielsen E (1982) The hydromagnetic oscillation of individual shells of the geomagnetic field. J Geophys Res 87:10432–10438

Poulter EM, Allan W, Bailey GJ (1988) ULF pulsation eigenperiods within the plasmasphere. Planet Space Sci 36: 185–196

Price IA, Waters CL, Menk FW, Bailey GJ, Fraser BJ (1999) A technique to investigate plasma mass density in the topside ionosphere using ULF waves. J Geophys Res 104:12723–12732

Prikryl P, Greenwald R, Sofko G, Villain J, Ziesolleck C, Friis-Christensen E (1998) Solar wind driven pulsed magnetic reconnection at the dayside magnetopause, Pc5 compressional oscillations, and field line resonances. J Geophys Res 103:17307–17322

Pu Z, Kivelson MG (1983) Kelvin-Helmholtz instability at the magnetopause: solution for compressible plasma. J Geophys Res 88:841–852

Rae IJ, Watt CEJ, Fenrich FR, Mann IR, Ozeke LG, Kale A (2007) Energy deposition in the ionosphere through a global field line resonance. Ann Geophys 25:2529–2539

Rankin R, Kabin K, Marchand R (2006) Alfvénic field line resonances in arbitrary magnetic field topology. Adv Space Res 38:1720–1729

Rauch J, Roux A (1982) Ray tracing of ULF waves in a multicomponent magnetospheric plasma: consequences for the generation mechanism of ion cyclotron waves. J Geophys Res 87:8191–8198

Rodger C, Thomson N, Dowden R (1996) A search for ELF/VLF activity associated with earthquakes using ISIS satellite data. J Geophys Res 101:13369–13378

Rodger CJ, Raita T, Clilverd MA, Seppälä A, Dietrich S, Thomson NR, Ulich T (2008) Observations of relativistic electron precipitation from the radiation

belts driven by EMIC waves. Geophys Res Lett. doi:10.1029/2008GL034804
Rother M, Schlegel K, Lühr H (2007) CHAMP observations of intense kilometer-scale field-aligned currents, evidence for an ionospheric Alfvén resonator. Ann Geophys 25:1603–1615
Russell CT, Luhmann JG, Odera TJ, Stuart WF (1983) The rate of occurrence of dayside Pc3,4 pulsations: The *L*-value dependence of the IMF cone angle effect. Geophys Res Lett 10:663–666
Sakaguchi K, Shiokawa K, Ieda A, Miyoshi Y, Otsuka Y, Ogawa T, Connors M, Donovan EF, Rich FJ (2007) Simultaneous ground and satellite observations of an isolated proton arc at subauroral latitudes. J Geophys Res. doi:10.1029/2006JA012135
Sakurai T, Tonegawa Y, Kitagawa T, Yumoto K, Yamomoto T, Kokubun S, Mukai T, Tsuruda T (1999) Dayside magnetopause Pc3 and Pc5 ULF waves observed by the GEOTAIL satellite. Earth Planets Space 51:965–978
Samson JC, Harrold BG, Ruohoniemi JM, Greenwald RA, Walker ADM (1992) Field line resonances associated with MHD waveguides in the magnetosphere. Geophys Res Lett 25:3701–3704
Samson JC, Waters CL, Menk FW, Fraser BJ (1995) Fine structure in the spectra of low latitude field line resonances. Geophys Res Lett 22:2111–2114
Santarelli L, Lepidi S, Cafarella L (2007) Propagation of low frequency geomagnetic field fluctuations in Antarctica: comparison between two polar cap stations. Ann Geophys 25:2405–2412
Sarris TE, Loto'aniu TM, Li X, Singer HJ (2007) Observations at geosynchronous orbit of a persistent Pc5 geomagnetic pulsation and energetic electron flux modulations. Ann Geophys 25:1653–1667
Sarris TE et al (2009a)Characterization of ULF pulsations by THEMIS. Geophys Res Lett. doi:10.1029/2008GL036732
Sarris TE, Li X, Singer HJ (2009b) A long-duration narrowband Pc5 pulsation. J Geophys Res. doi:10.1029/2007JA012660
Sarris TE, Wright AN, Li X (2009c) Observations and analysis of Alfvén wave phase mixing in the Earth's magnetosphere. J Geophys Res. doi:10.1029/2008JA013606
Schäfer S, Glassmeier KH, Eriksson PTI, Pierrard V, Fornaçon KH, Blomberg LG (2007) Spatial and temporal characteristics of poloidal waves in the terrestrial plasmasphere: a CLUSTER study. Ann Geophys 25:1011–1024
Schäfer S, Glassmeier KH, Eriksson PTI, Pierrard V, Fornaçon KH, Blomberg LG (2008) Spatio-temporal structure of a poloidal Alfvén wave detected by Cluster adjacent to the dayside plasmapause. Ann Geophys 26:1805–1817
Schulz M (1996) Eigenfrequencies of geomagnetic field lines and implications for plasma density modeling. J Geophys Res 101:17385–17397
Schwartz SJ, Burgess D, Moses JJ (1996) Low frequency waves in the Earth's magnetosheath: present status. Ann Geophys 14:1134–1150
Sciffer MD, Waters CL (2002) Propagation of ULF waves through the ionosphere: Analytic solutions for oblique magnetic fields. J Geophys Res. doi:10.1029/2001JA000184
Sciffer MD, Waters CL, Menk FW (2004) Propagation of ULF waves through the ionosphere: inductive effect for oblique magnetic fields. Ann Geophys 22:1155–1169
Sciffer MD, Waters CL, Menk FW (2005) A numerical model to investigate the polarisation azimuth of ULF waves through an ionosphere with oblique magnetic fields. Ann Geophys 23:3457–3471
Seyler CE, Liu K (2007) Particle energization by oblique inertial Alfvén waves in the auroral region. J Geophys Res. doi:10.1029/2007JA012412
Shprits Y (2009) Potential waves for pitch-angle scattering of near-equatorially mirroring energetic electrons due to the violation of the second adiabatic invariant. Geophys Res Lett. doi:10.1029/2009GL038322
Shprits Y, Elkington SR, Meredith NP, Subbotin DA (2008a) Review of modelling of losses and sources of relativistic electrons in the outer radiation belt I: radial transport. J Atmos Sol Terr Phys 70:1679–1693
Shprits Y, Subbotin DA, Meredith NP, Elkington SR (2008b) Review of modelling and losses of relativistic electrons in the outer radiation belt II: local acceleration and loss. J Atmos Sol Terr Phys 70:1694–1713
Sibeck DG, Korotova GI (1996) Occurrence patterns for transient magnetic field signatures at high latitudes. J Geophys Res 101:13413–13428
Singer HJ, Southwood DJ, Walker RJ, Kivelson MG (1981) Alfven wave resonances in a realistic magnetospheric magnetic field geometry. J Geophys Res 86:4589–4596
Skone S (2009) Using GPS TEC measurements to detect geomagnetic Pc 3 pulsations. Radio Sci. doi:10.1029/2008 RS004106
Smirnova NA, Hayakawa M (2007) Fractal characteristics of the ground-observed ULF emissions in relation to geomagnetic and seismic activities. J Atmos Sol Terr Phys 69:1833–1841
Spasojević M, Frey HU, Thomsen MF, Fuselier SA, Gary SP, Sandel BR, Inan US (2004) The link between a detached subauroral proton arc and a plasmaspheric plume. Geophys Res Lett. doi:10.1029/2003GL018389
Stephenson JA, Walker ADM (2002) HF radar observations of Pc5 ULF pulsations driven by the solar wind. J Geophys Res. doi:10.1029/2001GL014291
Summers D, Ni B, Meredith NP (2007) Timescales for radiation belt electron acceleration and loss due to resonant wave-particle interactions: 2. Evaluation for VLF chorus, ELF hiss, and electromagnetic ion cyclotron waves. J Geophys Res. doi:10.1029/2006JA011993
Sutcliffe P, Poole A (1989) Ionospheric Doppler and electron velocities in the presence of ULF waves. J Geophys Res 94:13505–13514
Takagi K, Hashimoto C, Hasegawa H, Fujimoto M, Tan-Dokoro R (2006) Kelvin-Helmholtz instability in a magnetotail flank-like geometry: three-dimensional MHD simulations. J Geophys Res. doi:10.1029/2006JA011631
Takahashi K, Denton RE (2007) Magnetospheric seismology using multi-harmonic toroidal waves observed at geosynchronous orbit. J Geophys Res. doi:10.1029/2006JA011709
Takahashi K, Ukhorskiy AY (2007) Solar wind control of Pc5 power at geosynchronous orbit. J Geophys Res. doi:10.1029/2007JA012483
Takahashi K, Ukhorskiy AY (2008) Timing analysis of the relationship between solar wind parameters and geosynchronous Pc5 amplitude. J Geophys Res. doi:10.1029/2008JA013327

Takahashi K, McPherron R, Terasawa T (1984) Dependence of the spectrum of Pc 3-4 pulsations on the interplanetary magnetic field. J Geophys Res 89:2770–2780
Takahashi K, Higbie P, Baker D (1985) Azimuthal propagation and frequency characteristic of compressional Pc 5 waves observed at geostationary orbit. J Geophys Res 90:1473–1485
Takahashi K, Denton RE, Anderson RR, Hughes WJ (2004) Frequencies of standing Alfvén wave harmonics and their implication for plasma mass distribution along geomagnetic field lines: statistical analysis of CRRES data. J Geophys Res. doi:10.1029/2003JA010345
Takahashi K, Liou K, Yumoto K, Kitamura K, Nosé M, Honary F (2005) Source of Pc4 pulsations observed on the nightside. J Geophys Res. doi:10.1029/2005JA011093
Takahashi K, Chi PJ, Denton RE, Lysak RL (eds) (2006) Magnetospheric ULF waves: synthesis and new directions. American Geophysical Union, Washington, DC, 359 pp
Takahashi K, Ohtani S, Denton RE, Hughes WJ, Anderson RR (2008) Ion composition in the plasma trough and plasma plume derived from a Combined Release and Radiation Effects Satellite magnetoseismic study. J Geophys Res. doi:10.1029/2008JA013248
Takahashi K, Berube D, Lee D-H, Goldstein J, Singer HJ, Honary F, Moldwin MB (2009) Possible evidence of virtual resonance in the dayside magnetosphere. J Geophys Res. doi:10.1029/2008JA013898
Tanaka Y-M, Yumoto K, Yoshikawa A, Itonaga M, Shinohara M, Takasaki S, Fraser BJ (2007) Horizontal amplitude and phase structure of low-latitude Pc 3 pulsations around the dawn terminator. J Geophys Res. doi:10.1029/2007JA012585
Tepley L, Landshoff RK (1966) Waveguide theory for ionospheric propagation of hydromagnetic emissions. J Geophys Res 71:1499–1504
Teramoto M, Nosé M, Sutcliffe PR (2008) Statistical analysis of Pi2 pulsations inside and outside the plasmasphere observed by the polar orbiting DE1 satellite. J Geophys Res. doi:10.1029/2007JA012740
Trakhtengerts VY, Demekhov AG (2007) Generation of Pc1 pulsations in the regime of backward wave oscillator. J Atmos Sol Terr Phys 69:1651–1656
Troitskaya VA (1961) Pulsation of the Earth′s electromagnetic field with periods of 1 to 15 seconds and their connection with phenomena in the high atmosphere. J Geophys Res 66:5–18
Troitskaya VA, Gul'yel'mi AV (1967) Geomagnetic micropulsations and diagnostics of the magnetosphere. Space Sci Rev 7:689–768
Troitskaya VA, Gul'yel'mi AV (1970) Hydromagnetic diagnostics of plasma in the magnetosphere. Ann Geophys 26:893
Troitskaya VA, Plyasova-Bakunina TA, Gul'yel'mi AV (1971) Connection of Pc2-4 pulsations with interplanetary magnetic field. Doklady Akad Nauk SSSR 197:1312
Turkakin H, Marchaud R, Kale ZC (2008) Mode trapping in the plasmasphere. J Geophys Res. doi:10.1029/2008JA013045
Ukhorskiy AY, Sitnov MI (2008) Radial transport in the outer radiation belt due to global magnetospheric compressions. J Atmos Sol Terr Phys. doi:10.1016/j.jastp.2008.07.018
Ukhorskiy AY, Takahashi K, Anderson BJ, Korth H (2005) Impact of toroidal ULF waves on the outer radiation belt electrons. J Geophys Res. doi:10.1029/2005JA011017
Ukhorskiy AY, Anderson BJ, Takahashi K, Tsyganenko NA (2006) Impact of ULF oscillations in solar wind dynamic pressure on the outer radiation belt electrons. Geophys Res Lett. doi:10.1029/2005GL024380
Usanova ME, Mann IR, Rae IJ, Kale ZC, Angelopolous V, Bonnell JW, Glassmeier K-H, Auster HU, Singer HJ (2008) Multipoint observations of magnetospheric compression-related EMIC waves by THEMIS and CARISMA. Geophys Res Lett. doi:10.1029/2008GL034458
Vellante M, Förster M (2006) Inference of the magnetospheric plasma mass density from field line resonances: a test using a plasmasphere model. J Geophys Res. doi:10.1029/2005JA011588
Vellante M, Förster M, Villante U, Zhang TL, Magnes W (2007) Solar activity dependence of geomagnetic field line resonance frequencies at low latitudes. J Geophys Res. doi:10.1029/2006JA011909
Viall NM, Kepko L, Spence HE (2009) Relative occurrence rates and connection of discrete frequency oscillations in the solar wind density and dayside magnetosphere. J Geophys Res. doi:10.1029/2008JA013334
Villante U (2007) Ultra low frequency waves in the magnetosphere. In: Kamide Y, Chian A (eds) Handbook of the solar-terrestrial environment. Springer, Berlin, Heidelberg, pp 397–422
Villante U, Lepidi S, Francia P, Meloni A, Palangio P (1997) Long period geomagnetic field fluctuations at Terra Nova Bay (Antarctica). Geophys Res Lett 24:1443–1446
Villante U, Francia P, Vellante M, Di Giuseppe P, Nubile A, Piersanti M (2007) Long period oscillations at discrete frequencies: a comparative analysis of ground, magnetospheric and interplanetary observations. J Geophys Res. doi:10.1029/2006JA011896
Volwerk M et al (2007) Flow burst-induced Kelvin-Helmholtz waves in the terrestrial magnetotail, Geophys Res Lett. doi:10.1029/2007GL029459
Walker ADM (1981) The Kelvin-Helmholtz instability in the low-latitude boundary layer. Planet Space Sci 29:1119–1133
Walker ADM (2000) Reflection and transmission at the boundary between two counterstreaming MHD plasmas – active boundaries or negative-energy waves? J Plasma Phys 63:203–219
Walker ADM (2005) Magnetohydrodynamic waves in geospace – the theory of ULF waves and their interaction with energetic particles in the solar-terrestrial environment. IOP Publishing, Bristol, 550 pp
Waters CL, Sciffer MD (2008) Field line resonant frequencies and ionospheric conductance: results from a 2D MHD model. J Geophys Res. doi:10.1029/2007JA012822
Waters CL, Cox SP (2009) ULF wave effects on high frequency signal propagation through the ionosphere. Ann Geophys 27:2779–2788
Waters CL, Menk FW, Fraser BJ (1991) The resonance structure of low latitude Pc3 geomagnetic pulsations. Geophys Res Lett 18:2293–2296
Waters CL, Menk FW, Fraser BJ (1994) Low latitude geomagnetic field line resonance: experiment and modeling. J Geophys Res 99:17547–17558
Waters CL, Samson JC, Donovan EF (1995) The temporal variation of the frequency of high-latitude field line resonances. J Geophys Res 100:7987–7996

Waters CL, Samson JC, Donovan EF (1996) Variation of plasmatrough density derived from magnetospheric field line resonances. J Geophys Res 101:24737–24745

Waters CL, Harrold BG, Menk FW, Samson JC, Fraser BJ (2000) Field line resonances and waveguide modes at low latitudes 2. A model. J Geophys Res 105:7763–7774

Waters CL, Sciffer MD, Fraser BJ, Brand K, Foulkes K, Menk FW, Saka O, Yumoto K (2001) The phase structure of very low latitude ULF waves across dawn. J Geophys Res 106:15599–15607

Waters CL, Takahashi K, Lee D-H, Anderson BJ (2002) Detection of ultra-low-frequency cavity modes using spacecraft data. J Geophys Res. doi:10.1029/2001JA000224

Waters CL, Menk FW, Thomsen MF, Foster C, Fenrich FR (2006) Remote sensing the magnetosphere using ground based observations of ULF waves. In: Takahashi K, Chi PJ, Denton RE, Lysak RL (eds) Magnetospheric ULF waves: synthesis and new directions. American Geophysical Union, Washington, DC, pp 319–337

Waters CL, Yeoman TK, Sciffer MD, Ponomarenko P, Wright DM (2007) Modulation of radio signals by ULF waves. Ann Geophys 25:1113–1124

Webster DJ, Fraser BJ (1985) Source regions of low-latitude Pc1 pulsations and their relationship to the plasmapause. Planet Space Sci 33:777–793

Wentworth RC (1964) Enhancement of hydromagnetic emissions after geomagnetic storms. J Geophys Res 69:2291–2298

Wild JA, Yeoman TK, Waters CL (2005) Revised time-of-flight calculations for high-latitude geomagnetic pulsations using a realistic magnetospheric magnetic field model. J Geophys Res. doi:10.1029/2004JA010964

Wright DM, Yeoman TK (1999) High-latitude HF Doppler observations of ULF waves: 2. Waves with small spatial scale sizes. Ann Geophys 17:868–876

Wright AN, Mann IR (2006) Global MHD eigenmodes of the outer magnetosphere. In: Takahashi K, Chi PJ, Denton RE, Lysak RL (eds) Magnetospheric ULF waves: synthesis and new directions. American Geophysical Union, Washington, DC, pp 51–72

Wright AN, Allan W (2008) Simulations of Alfvén waves in the geomagnetic tail and their auroral signatures. J Geophys Res. doi:10.1029/2007JA012464

Wright DM, Yeoman TK, Jones TB (1999) ULF wave occurrence statistics in a high latitude HF Doppler sounder. Ann Geophys 17:749–759

Yahnin AG, Yahnina TA (2007) Energetic proton precipitation related to ion-cyclotron waves. J Atmos Sol Terr Phys 69:1690–1706

Yahnin AG, Yahnina TA, Frey HU (2007) Subauroral proton spots visualize the Pc1 source. J Geophys Res. doi:10.1029/2007JA012501

Yarker JM, Southwood DJ (1986) The effect of non-uniform ionospheric conductivity on standing magnetospheric Alfvén waves. Planet Space Sci 34:1213–1221

Yearby KH, Clilverd MA (1996) Doppler shift pulsations on whistler mode signals from a VLF transmitter. J Atmos Sol Terr Phys 58:1489–1496

Yeoman T, Wright D, Chapman P, Stockton-Chalk A (2000) High-latitude observations of ULF waves with large azimuthal wavenumbers. J Geophys Res 105:5453–5462

Yumoto K, Saito T (1983) Relation of compressional hm waves at Goes 2 to low-latitude Pc 3 magnetic pulsations. J Geophys Res 88:10041–10052

Yumoto K, Saito T, Akasofu SI, Tsurutani B, Smith E (1985) Propagation mechanism of daytime Pc 3-4 pulsations observed at synchronous orbit and multiple ground-based stations. J Geophys Res 90:6439–6450

Ziesolleck CWS, McDiarmid DR (1994) Auroral latitude Pc5 field line resonances; quantized frequencies, spatial characteristics, and diurnal variations. J Geophys Res 99:5817–5830

Zong QG et al (2007) Ultralow frequency modulation of energetic particles in the dayside magnetosphere. Geophys Res Lett. doi:10.1029/2007GL029915

Zong QG et al (2009) Energetic electron response to ULF waves induced by interplanetary shocks in the outer radiation belt. J Geophys Res. doi:10.1029/2009JA014393